(2) LEVEL II

AFAPL-TR-79-2041

AD A076257

PROBE EFFECTS IN GAS TURBINE COMBUSTOR EMISSIONS MEASUREMENTS

J. A. Clark
J. E. Peters
A. M. Mellor

The Combustion Laboratory
School of Mechanical Engineering
Purdue University
West Lafayette, Indiana 47907

JUNE 1979

FINAL REPORT March 1978 - October 1978

AIR FORCE AERO PROPULSION LABORATORY
AIR FORCE WRIGHT AERONAUTICAL LABORATORIES
AIR FORCE SYSTEMS COMMAND
WRIGHT-PATTERSON AIR FORCE BASE, OHIO 45433

NOTICE

When Government drawings, specifications, or other data are used for any purpose other than in connection with a definitely related Government procurement operation, the United States Government thereby incurs no responsibility nor any obligation whatsoever; and the fact that the government may have formulated, furnished, or in any way supplied the said drawings, specifications, or other data, is not to be regarded by implication or otherwise as in any manner licensing the holder or any other person or corporation, or conveying any rights or permission to manufacture, use, or sell any patented invention that may in any way be related thereto.

This report has been reviewed by the Information Office (OI) and is releasable to the National Technical Information Service (NTIS). At NTIS, it will be available to the general public, including foreign nations.

This technical report has been reviewed and is approved for publication.

W. M. Roquemore
Name

W. M. Roquemore
Project Engineer

Arthur V. Churchill
Name

Arthur V. Churchill
Chief, Fuels Branch

FOR THE COMMANDER

Blackwell C. Dunnam
Name

Blackwell C. Dunnam
Chief, Fuels and Lubrication Division

"If your address has changed, if you wish to be removed from our mailing list, or if the addressee is no longer employed by your organization please notify AFAPL/SFF ,W-PAFB, OH 45433 to help us maintain a current mailing list".

Copies of this report should not be returned unless return is required by security considerations, contractual obligations, or notice on a specific document.

AIR FORCE/86780/7 September 1979 — 230

SECURITY CLASSIFICATION OF THIS PAGE *(When Data Entered)*

REPORT DOCUMENTATION PAGE

READ INSTRUCTIONS BEFORE COMPLETING FORM

1. REPORT NUMBER: AFAPL-TR-79-2041	2. GOVT ACCESSION NO.
3. RECIPIENT'S CATALOG NUMBER	
4. TITLE *(and Subtitle)*: PROBE EFFECTS IN GAS TURBINE COMBUSTOR EMISSIONS MEASUREMENTS	5. TYPE OF REPORT & PERIOD COVERED: Final Rept. 1 Mar [redacted] - 1 Oct [redacted] 78
	6. PERFORMING ORG. REPORT NUMBER: PURDU-CL-78-05
7. AUTHOR(s): J.A. Clark, J.E. Peters, A.M. Mellor	8. CONTRACT OR GRANT NUMBER(s): F33615-77-C-2069
9. PERFORMING ORGANIZATION NAME AND ADDRESS: Purdue University, The Combustion Laboratory, School of Mechanical Engineering, West Lafayette, Indiana 47907	10. PROGRAM ELEMENT, PROJECT, TASK AREA & WORK UNIT NUMBERS: 2308-57-06
11. CONTROLLING OFFICE NAME AND ADDRESS: Air Force Aero Propulsion Laboratory (SFF) Wright-Patterson	12. REPORT DATE: Jun [redacted] 79 13. NUMBER OF PAGES: 59
14. MONITORING AGENCY NAME & ADDRESS *(if different from Controlling Office)*	15. SECURITY CLASS. *(of this report)*: Unclassified 15a. DECLASSIFICATION/DOWNGRADING SCHEDULE

16. DISTRIBUTION STATEMENT *(of this Report)*

Approved for public release; distribution unlimited.

17. DISTRIBUTION STATEMENT *(of the abstract entered in Block 20, if different from Report)*

18. SUPPLEMENTARY NOTES

This research was funded by the Air Force Aero-Propulsion Laboratory (AFAPL) via the Senior Investigator Program through the University of Dayton under purchase orders RI83738 and RI85195.

19. KEY WORDS *(Continue on reverse side if necessary and identify by block number)*

Gas Sampling Probes	Carbon Monoxide	Oxides of Nitrogen
Emissions Probes	Unburned Hydrocarbons	Nitric Oxide
Aircraft Pollutants	Total Hydrocarbons	

20. ABSTRACT *(Continue on reverse side if necessary and identify by block number)*

Four geometrically distinct, stainless steel probes are used to study the concentrations of CO, HC, NO, and NOX at several different radial and two different axial positions within a simplified gas turbine combustor. The probes are all water cooled but do not employ an aerodynamic quench. They are designed to assess the effect of tip shape, tip to body proximity, and probe entry point on measured pollutant concentrations.
(continued on reverse side)

DD FORM 1 JAN 73 1473 EDITION OF 1 NOV 65 IS OBSOLETE

Unclassified

SECURITY CLASSIFICATION OF THIS PAGE *(When Data Entered)*

105 350

20. ABSTRACT (continued)

Though probe entry point and tip to body proximity are shown to imperceptibly affect the pollutant concentrations, probe tip geometry has a marked impact on the measured pollutant levels. Specifically, the aerodynamic, tapered-tip probe yields depressed CO and HC, and elevated NO concentrations compared to the other three blunt-tipped probes.

Regarding reproducibility, the pollutant concentrations measured with one of the blunt-tipped probes in this study are compared to pollutant levels measured with the same probe three years ago (Tuttle et al. 1975). CO and HC are shown to be the most reproducible species, while NO and NOX acceptably but less accurately agree with past studies.

PREFACE

Any gas turbine combustor experiment requires the cooperation of many people not only to operate the combustor, but also to maintain the equipment, and reduce the data to meaningful numbers. The authors thank the following persons for their help in this study: Doug Danley, Larry Eckstein, Professor Colin Ferguson, Tab Heffernan, Paul Leonard, Tom Miller, Dave Ramsey and Bill Wyatt.

This research was funded by the Air Force Aero-Propulsion Laboratory (AFAPL) via the Senior Investigator Program through the University of Dayton under purchase orders RI83738 and RI85195. The authors appreciate the guidance of Royce Bradley and Dr. Mel Roquemore of the Fuels Branch at AFAPL.

TABLE OF CONTENTS

LIST OF ILLUSTRATIONS

LIST OF TABLES

SECTION I

INTRODUCTION AND SUMMARY

Probe geometry effects on pollutant concentration measurements in a simplified gas turbine combustor are explored in this study. The combustor operating conditions are the same as those used by Tuttle et al. (1975) in a program which did not include probe geometry variations. Tuttle et al. (1975) selected their operating conditions as being representative of a gas turbine running at a cruise condition. The reason for repeating Tuttle's flame in the present study is to determine the accuracy of reproducing Tuttle's results using Tuttle's probe.

Four stainless steel water cooled probes, none employing aerodynamic quench, have been constructed for this experiment. Three of the probes have blunt tips while a fourth has a more aerodynamic, tapered tip. Also, three probes (not the same three) have bodies well removed from their tips, while a fourth has a body and tip in close proximity. Finally, three probes are inserted through the window holes along the side of the combustor, but a fourth probe is inserted axially from a point farther downstream. These geometry variations should be suitable for measuring the effect of tip shape, tip to body proximity and probe entry point on gas turbine pollutant concentrations. More detailed descriptions and drawings of the probes are provided in the section entitled Experimental Apparatus.

The results of this study basically show that the pollutant concentrations reported by Tuttle et al. (1975) can be reproduced in varying degrees, depending on the pollutant. Carbon monoxide (CO) concentrations along with unburned hydrocarbons (HC) show the most reproducible profiles, while nitric oxide (NO) and NO_x ($NO + NO_2$) are less reproducible species. Examination of the pollutant profiles reveals that the minimum error in the reproduction of pollutant concentrations in a gas turbine combustor is 10%. Though such an error would not be acceptable for turbulence measurements, it is suitable for a combustor liner design engineer.

As for probe geometry variation, there is no detectable effect on pollutant concentrations of tip to body proximity or probe insertion point, within the scatter. This lack of effect can be explained in two ways. First, the constantly changing flame shape and flow pattern in a high intensity turbulent diffusion flame are accompanied by fluctuations in species concentration. These fluctuations show up as data scatter which erases these two probe geometry effects. Second, since the thin shear layer of the flowfield is typically characterized by large species concentration gradients, a minor uncertainity in probe tip position can again result in data scatter which wipes out any changes in pollutant concentration due to either tip-body proximity or probe insertion point.

In contrast, probe tip geometry seems to have a measurable effect on pollutant concentrations. In particular, the tapered tip probe results in HC and CO concentrations which are consistently lower than those obtained using the other three probes. Also, the NO concentrations

obtained from the tapered tip probe located 2.54 cm downstream of the flameholder are much higher than the NO concentrations from any other probe. There seem to be two possible explanations for these differences. First, it is possible that the flowfield near the tapered tip is significantly different than the flowfield near the blunt tip, thus altering measured pollutant concentrations. Another possibility is that the uncooled probe tip prevents immediate quenching of reactions within the probe. This lack of quenching would explain the depressed levels of CO and HC and increased NO.

It should be noted that the pollutant concentrations measured using the tapered tip probe cannot be judged as "right" or "wrong" merely because those concentrations differ from those obtained with other probes. One method of determining the accuracy of the results from all the probes involves in situ optical measurements. Laser methods such as coherent anti-Stokes Raman scattering could be used not only to verify the pollutant concentrations measured by the probes, but also to measure the change in pollutant concentration due to the presence (or absence) of a probe.

The remainder of this report contains a literature review, a description of the experimental apparatus, the results of this study and its conclusions. The Appendix contains the experimental results in tabular form.

SECTION II

LITERATURE REVIEW

Many of the numerous studies pertaining to the quantitative measurement of pollutants in hydrocarbon-air flames have concentrated on the oxides of nitrogen. This attention to NO_x ($NO + NO_2$) has been due in part to a desire to minimize engine exhaust concentrations of these oxides in order to control air pollution. Also, several early investigators using sampling probes obtained conflicting experimental results, and these contradictions promoted further research. Finally, it has been assumed that the other two major pollutants (HC and CO) can be accurately sampled and measured, provided they are adequately quenched in the sampling probe.

Previous to 1970, it was assumed that the NO_2 contribution to NO_x in flames was negligible due to consideration of the equilibrium constant for the reaction $2NO + O_2 \rightarrow 2NO_2$. LaPointe and Schultz (1971) sampled gases within a low pressure model gas turbine combustor using a water cooled probe with an orifice at the tip (for aerodynamic quenching) and found that in all but a few locations NO constituted at least 95% of the NO_x. A chemiluminescent analyzer was used in their work.

Later, England et al. (1973) probed a methane fired furnace with both cooled and uncooled stainless steel probes. They found only small differences in measured NO between the two probes for equivalence ratios $\phi<.7$. However, for $\phi>.7$ the water cooled probe yielded

substantially higher (>40%) amounts of NO than did the uncooled probe. Their explanation was that the uncooled probe allowed the $2NO \rightarrow N_2 + O_2$ reaction, while the cooled probe did not. That same year, Schefer et al. (1973) also examined the differences in measured NO and NO_2 in cooled and uncooled probes, all with aerodynamic quenching. Two flames were studied: an opposed jet flame, and a turbulent diffusion flame. The oxides of nitrogen were detected using a chemiluminescent analyzer, whose catalyst for converting NO_2 to NO was molybdenum heated to $500^{o}C$. For the opposed jet flame, the NO readings for gases from the cooled probes were much lower than the readings of NO for gases from the uncooled probes, even though the NO_x readings from the two probes were the same. Their explanation was that the cooled probes prevented the catalyzed reaction $NO_2 \rightarrow NO + O$ in the probe. For the turbulent diffusion flame, differences in NO and NO_x in the gases from the cooled and uncooled probes were insignificant. They reasoned that the uncooled probes had not been heated sufficiently to allow the catalyzed reaction $NO_2 \rightarrow NO + O$. They concluded that the NO_2 constituted as much as 80% of the NO_x in the opposed jet flame. Even though Schefer et al. (1973) did examine the rich regions of the turbulent diffusion flame, they found no dependence of NO and NO_x readings on whether or not the probes were cooled. Thus, their findings did not substantiate those of England et al. (1973). Schefer et al. (1973) explained this inconsistency by pointing out the fact that the probes of England et al. (1973) did not use aerodynamic quenching.

Tuttle, Shisler, and Mellor (1974) reviewed the NO/NO_2 controversy, and included detailed descriptions and comparisons of the chemiluminescent and non-dispersive ultraviolet analyzer (NDUV) techniques for detecting NO_2. They discussed chemiluminescent converter catalyst problems and made several recommendations concerning the conditions and check-out of the converter. Their conclusion, which was based in part on their own experimental work with cooled stainless steel probes and chemiluminescent and NDUV analyzers, was that the question as to whether NO_2 is being formed or destroyed in the sampling lines could not be easily resolved. They allowed that the observation of NO_2 by some investigators and not by others could well be attributed to differing experimental techniques.

Laurendeau (1975) showed that .1 msec were required to oxidize 23% of the NO to NO_2 for a reacting mixture of oxygen and nitrogen at $700^{o}K$ and 5 atm. He observed that this time was short enough to allow formation of NO_2, particularly if an NO/O mixture were rapidly quenched. He pointed out that this rapid quenching is the probable situation in a gas turbine combustor, where turbulence, bulk convection and recirculation promote movement of radical species to cooler regions. Furthermore, Laurendeau opined that the interaction of cool primary air jets with hot recirculation zone gases offered the best conditions for NO_2 formation. Another reaction which would promote NO_2 formation is $NO + HO_2 \rightarrow NO_2 + OH$. This reaction was ignored in previous kinetic models, and was not considered by Laurendeau (1975).

That same year, Allen (1975) studied NO and NO_x above a premixed methane-air flame on a Botha-Spalding burner. Gases were withdrawn through an uncooled fine orifice silica probe and the products were analyzed using a chemiluminescence analyzer, a galvanic cell detector, and a Griess-Saltzman reagent. Allen (1975) found that the NO_x in the visible flame zone appeared to be predominately NO_2, but he believed the NO_2 was generated in the probe rather than being present in the combustion zone. He explained that the contact of the sample gases with the probe wall caused the rapid quenching of NO and O in the sample, promoting the reaction $NO + O \rightarrow NO_2$. Allen (1975) referred to the paper by Schefer et al. (1973) in which the NO from cooled probes in an opposed jet flame was much lower than the NO from uncooled probes. Allen disagreed with the authors, who concluded that the NO_2 was present in the flame and that the cooled probes were more accurate because they quenched the $NO_2 \rightarrow NO + O$ reaction. Allen argued that the rapid quenching of the cooled probes caused NO_2 formation and that the results from uncooled probes were probably more accurate. Allen did report that total NO_x was unaffected by sampling method and was therefore probably conserved.

Hilliard and Wheeler (1977) dealt with the catalyzed oxidation of nitric oxide to nitrogen dioxide, especially concerning themselves with the catalytic effect of stainless steel, since it is commonly used in sampling probes. They found that type 316 stainless steel strongly promotes the $NO \rightarrow NO_2$ reaction, and that the chromium in the stainless

steel was the catalyst. Furthermore, they stated that the most rapid catalysis of NO oxidation takes place near 600°C and noted that this temperature was quite close to the temperature of a chemiluminescent analyzer converter, whose purpose is to promote the opposite reaction. Hilliard and Wheeler (1977) suggested that chemiluminescent analyzer converters should use a molybdenum catalyst, which has been used by commercial instrumentation manufacturers to catalyze the $NO_2 \rightarrow NO$ reaction at 400°C.

Benson and Samuelson (1977) found that NO_2 was reduced to NO in 316 stainless steel at temperatures exceeding 100°C in the presence of propylene, 200°C in the presence of ethylene, and 300°C in the presence of methane. Furthermore, they concluded that NO_x is removed in 316 stainless steel at temperatures exceeding 200°C in the presence of propylene and 300°C in the presence of ethylene.

Attempting to summarize several previous studies, Kramlich and Malte (1978) asserted that the best current estimate is that NO_2 is capable of forming both within the combustor and within the sample probe. They used both cooled and uncooled fine tipped quartz probes in a jet-stirred Longwell type reactor burning methane-air. They concluded, like Allen (1975), that the temperature quench of the cooled probes caused oxidation of NO to NO_2, when sampling from fuel-lean flames.

It appears that the measurement of NO and NO_2 in flames is strongly dependent on flame type, local equivalence ratio, probe material,

probe cooling, and analysis method. As Laurendeau (1975) points out, when relatively cold air impinges on a flame front, NO_2 will likely be formed. Kramlich and Malte (1978) assert that a flame without strong recirculation, large scale turbulence, and cold air jets is unlikely to form appreciable NO_2. Several investigators (for example, Tuttle et al., 1974) indicated the special problems of chemiluminescent analyzer converters when the sampling zone is fuel rich. Stainless steel and quartz probes have been both lauded and criticized for their possible distortion of NO and/or NO_2, and there is an equal amount of disagreement as to whether cooling the probe is beneficial or detrimental to accuracy. However, several authors agreed (among them Allen (1975)) that total NO_x is conserved in the probe provided the sample is kept below $200^{o}C$. Finally, though chemiluminescence is the most widely used detection method because of its sensitivity to low levels of NO, other detectors, such as the NDUV, are not subject to uncertainties concerning catalytic effects as is the chemiluminescent analyzer converter. One problem in using the NDUV is calibration. Mixtures of NO_2 in N_2 have a shelf life of less than six months because the NO_2 dissociates easily to form NO and O_2. Chemiluminescent analyzers do not have a calibration problem because the NO/N_2 mixture with which they are calibrated is relatively stable.

In closing, it should be mentioned that the accurate detection of HC and CO in flames almost certainly requires quenching and therefore a water-cooled probe. Though aerodynamic quenching has been used with

some success, it is not practical in a gas turbine combustor probe because soot constantly clogs the orifice or nozzle. Furthermore, at least one investigator, Seery et al. (1977), has found that the fine orifice-sudden expansion method of quenching can lead to a standing shock wave at the orifice, meaning that instead of being cooled, the sample gases are actually being heated for a short time as they pass through the orifice. Use of stainless steel as the probe material is almost mandatory if the probe is to survive in the severe combustion environment for any length of time. The next section describes the gas turbine combustor and the four probes used in this study.

SECTION III

EXPERIMENTAL APPARATUS

A. Facility Description

The experimental combustor for this study uses compressed air from a blowdown storage system. Maximum system pressure of 150 atm permits a maximum air flow rate of 4.5 kg/sec. The tunnel itself is actually composed of four sections, each with a separate function. Section one is an inlet flow control valve, which is used in conjunction with an orifice type flowmeter. Downstream of this valve is the preheating combustor in which liquid propane is burned to preheat the inlet air from room temperature up to a maximum of 950°K. This slave burner contains a standard Allison T-56 combustor with a duplex pressure atomizer, and supplies heated, vitiated air to the test section. Between the preheating and test sections, air temperature is monitored with a thermocouple rake mounted across the duct. This rake is actually a stainless steel bar, in which eight chromel-alumel thermocouples are positioned to yield an area averaged estimate of the air temperature. Also between the preheating and test sections, a gas sampling rake is used to extract test section inlet air samples for gas analysis (see Figure 1). This figure also shows that the gas flow leaving the test section is turned 45°. The resulting elbow provides a convenient opening through which a gas sampling probe may be inserted. For this study, gas sampling probes have also been inserted through the window holes of the test section. Finally, the gas flow passes through a movable,

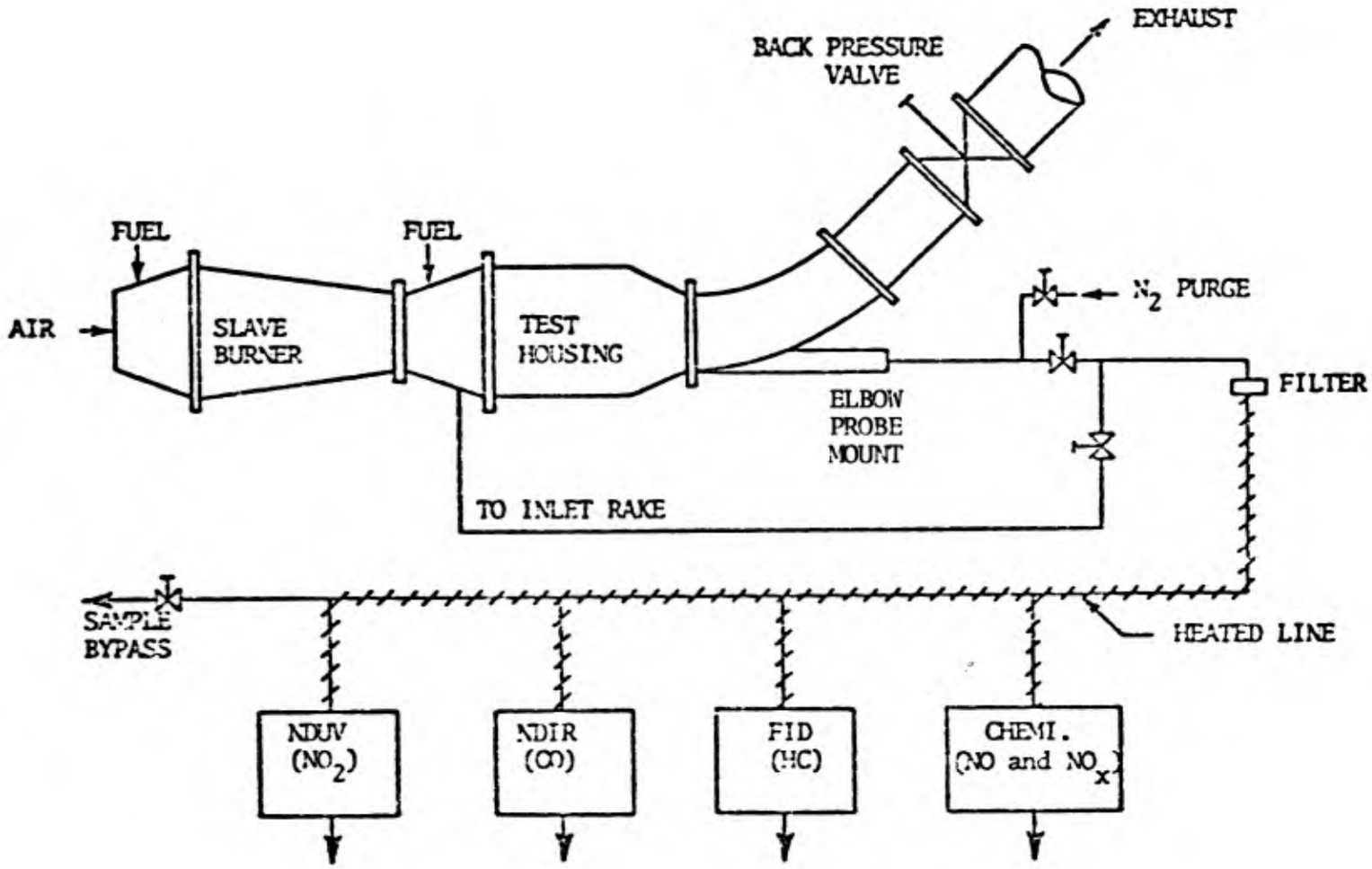

Figure 1. Schematic of the Experimental Apparatus

conically shaped back pressure valve which maintains test section pressure as desired between one and ten atmospheres. These four sections allow any one of the basic combustor operating parameters (inlet temperature, pressure, air flow rate, overall equivalence ratio) to be varied independently of the others. Since these operating conditions are hand-controlled, their day to day variations are probably greater than they would be if they were automatically controlled.

B. Test Section

The test section housing is stainless steel pipe of inner diameter 14.63 cm and wall thickness of 1.1 cm. Depicted in figure 2, five quartz windows are mounted 6.35 cm apart along the wall of the test section, allowing visual and physical access to the test section interior. Downstream of the windows, a reducing section is cooled by water in a cooling jacket, and near the end of the test section, water is injected into the gas flow to thermally protect the back pressure valve and muffler.

The flameholder is a circular disc (11.43 cm diameter) mounted flush with the edge of the first window, and a fuel pressure atomizer is located in the center of the disc. The atomizer is a Delavan #35-90 nozzle, meaning it is rated at 35 gal/hr (water) for an injection pressure of 125 psid and had a nominal spray angle of 90^{o}. The diameter of the flameholder and the nozzle size and angle have been selected to duplicate the flame studied by Tuttle et al. (1975). A cross section of the test section showing the disc, nozzle and access windows is shown in figure 3.

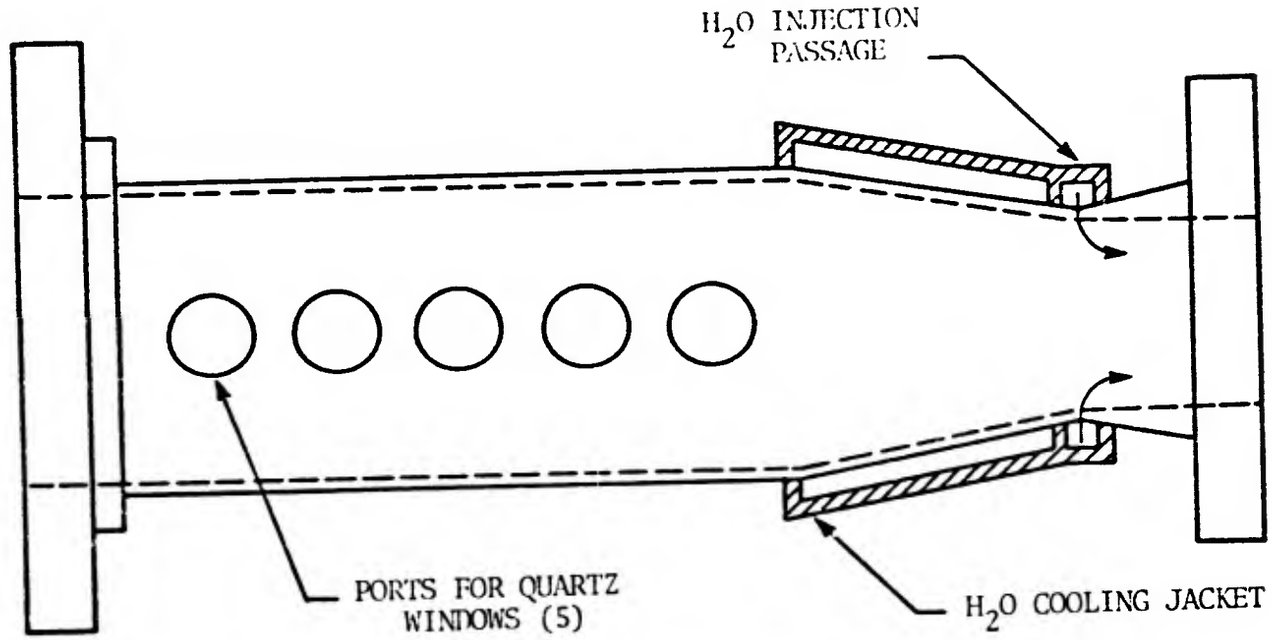

Figure 2. Test Section Housing Schematic

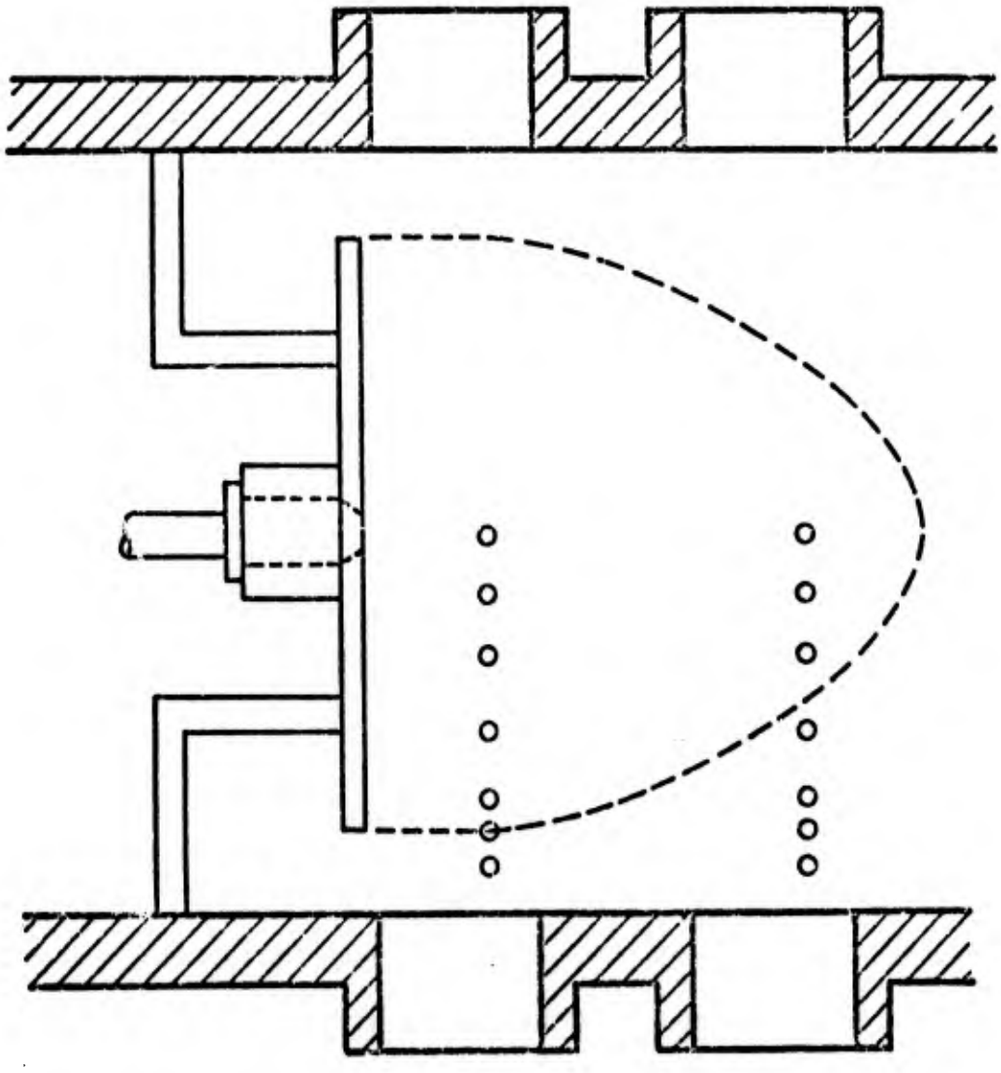

Figure 3. Cross Section of Combustor Showing Sampling Locations and Shear Layer

CL-1036

C. Gas Analysis System

Gas samples extracted from either the test section or the inlet gas rake are channeled to the gas analysis system (see Figure 1). The stainless steel sample lines use thermostatically controlled resistive heat tapes to prevent water condensation, and a heated glass fiber filter removes carbon particulates. The sample stream is analyzed on a continuous basis for concentrations of carbon monoxide, unburned hydrocarbons, nitric oxide and nitrogen dioxide using a nondispersive infrared analyzer (Beckman model 315A), a flame ionization detector (Beckman model 402) and a laboratory built chemiluminescent analyzer, respectively. Actually, the chemiluminescent analyzer equipped with a stainless steel $NO_2 \rightarrow NO$ converter allows monitoring of either NO or total $NO_x (NO + NO_2)$.

D. Probe Descriptions

Four geometrically distinct probes were used in this study to measure the effects of probe tip and probe body variations on measured pollutant concentrations. All four probes consist of three concentric stainless steel tubes, 9.5 mm, 6.4 mm, and 3.2 mm in diameter, respectively. The outer two tubes carry water to and from the probe tip, while the smallest tube carries sample gases. Probe outlet water temperature is monitored to insure rapid quenching. The hole in the probe tip is approximately the same diameter as the sampling tube. Though other investigators such as Schefer et al. (1973) have used aerodynamic

quenching, a fine orifice sampling hole is not used here to avoid the soot clogging problem as well as the possible complications due to a standing shock wave at the orifice. Thus, only the cool flowing water surrounding the sampling tube quenches reactions within the probe. Stainless steel probes are preferable to probes of other materials for durability reasons.

Probe #1 is the only one of the four which is inserted through the elbow downstream of the test section. By sliding this probe into or out of the elbow, the probe tip can be located at any axial position between the flameholder and the exhaust plane 29.2 cm downstream. The probe tip can also be located at any radial distance from the combustor centerline by rotating the probe body. Figure 4 shows how the probe tip and stem are parallel to but offset from the probe body to allow changes in the tip radial position through rotation of the probe body. The tip of this probe is blunt insuring adequate cooling (and therefore durability) of the tip material.

Probes #2, #3, #4 all have 90^{o} bends no more than 17.8 cm from their tips and are inserted through the window holes along the side of the test section. Probe #2 has a 17.8 cm stem length and, like probe #1, a blunt tip. Because of the stem length, this probe can only be mounted in the 4th or 5th window holes, meaning that the tip may only be located at two axial positions: 2.54 cm and 8.89 cm downstream of the flameholder. Radial position of probes #2, #3, #4 may be varied by moving the probe body into or out of the window hole. Thus, the

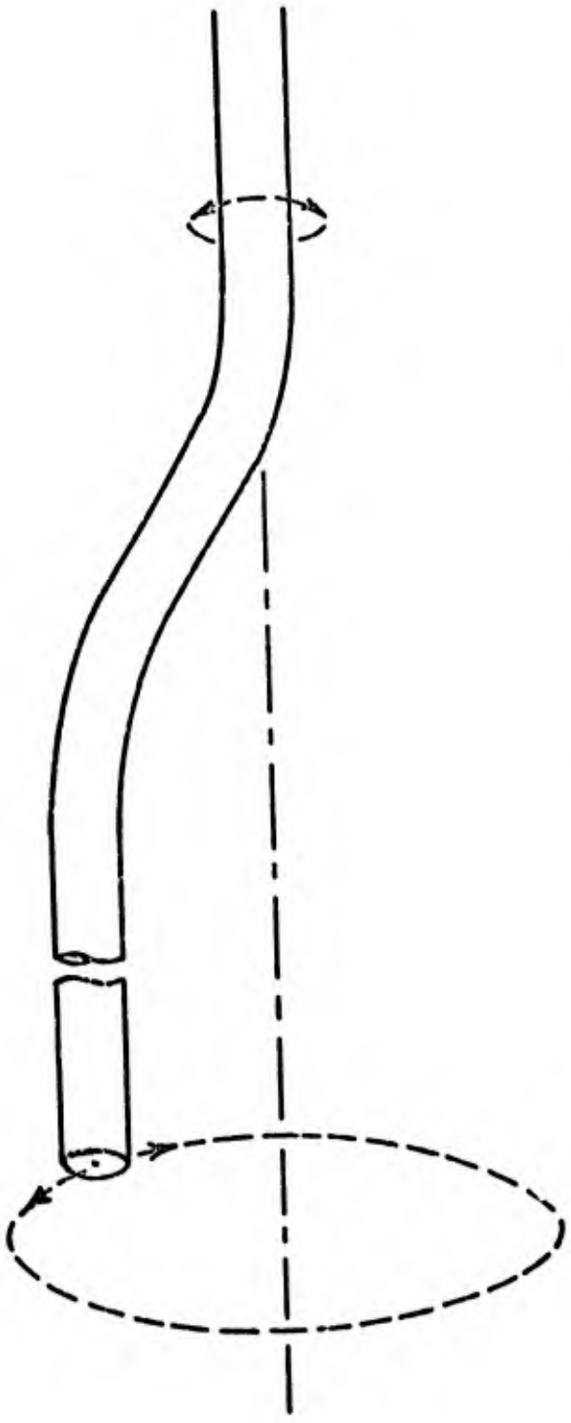

Figure 4. Partial Drawing of Probe #1 Showing How Tip Radial Position is Changed by Probe Rotation

probe tips may be located at any radial distance from the centerline. Figure 5 compares the possible tip radial positions for probe #1 and probes #2, #3, #4. To reiterate, all four probe tips may be located at any radial distance from the center line, but the tip of probe #1 does not trace out the same path as the tips of probes #2, #3, #4. The stem length of probe #2 has been chosen to allow the probe tip to be located more than fifteen diameters upstream of the probe body. Thus, it is likely that this side entry probe body has a negligible effect on pollutant concentrations measured with probe #2.

Probe #3 is like probe #2 except that its stem length is only 5.08 cm. Because of the short stem, probe #3 can be inserted into windows #2, #3, #4, or #5, meaning that the probe tip can be located at four different axial positions: 2.54 cm, 8.89 cm, 15.24 cm, and 24.13 cm downstream of the flameholder. To duplicate the probe #2 tip positions, probe #3 is only inserted into windows #2 or #3. The short stem length of probe #3 means that the probe tip is less than six diameters upstream of the side entry probe body, and thus, probe #3 has been designed to measure the effect of tip to body proximity on pollutant concentrations.

Probe #4 is like probe #2 except that is has a tapered tip. Again, since its stem length is 17.8 cm, it can only be inserted through windows #4 or #5. The tapered tip is difficult to cool, but it may disturb the surrounding flowfield less than the blunt tip used on the other three probes. This assumption of decreased flow disturbance

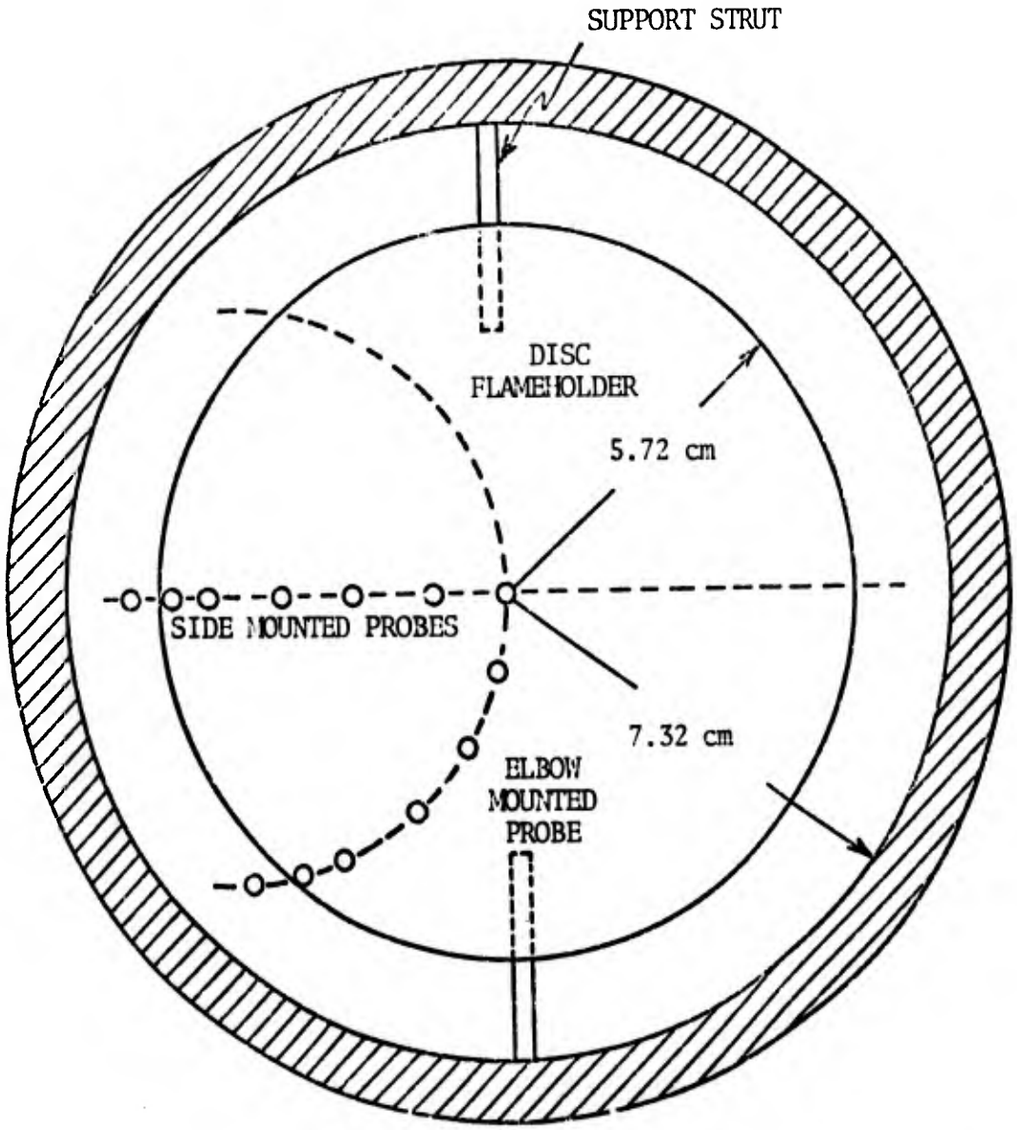

Figure 5. View inside combustor looking upstream and showing sampling points for side mounted and elbow mounted probes

CL-1038

depends on the assumption that the flow direction is parallel to the probe stem. The flow direction assumption is probably true at the 8.89 cm axial sampling location, but may not be true at the 2.54 cm sampling location because of the flow recirculation near the flameholder. Thus, probe #4 has been designed to measure the effect of tip geometry on pollutant concentrations. Figures 6 and 7 show the differences in stem length and tip design for probes #2, #3, #4.

As for uncertainties regarding tip location, probes #2, #3, #4 are much less subject to these inaccuracies than is probe #1. Because the side entry probes are always mounted in the center of a fixed window hole, the uncertainty in the axial position of their tips is negligible. Radially, these side entry probes can be positioned to an accuracy of ±.3 cm. Unlike the side entry probes, probe #1 can be located at any axial distance from the flameholder, but its radial position is more subject to error than the side entry probes. This positioning error is due to the fact that the support point of the probe is located far from the tip, causing considerable flexing of the probe and constant fluctuations of the probe tip during combustor operation. In fact, fluctuations as large as ±1 cm have occasionally been observed when the tip is close to the flameholder. These fluctuations are not seen with the side entry probes because the probe tips are fairly close to the probe support points.

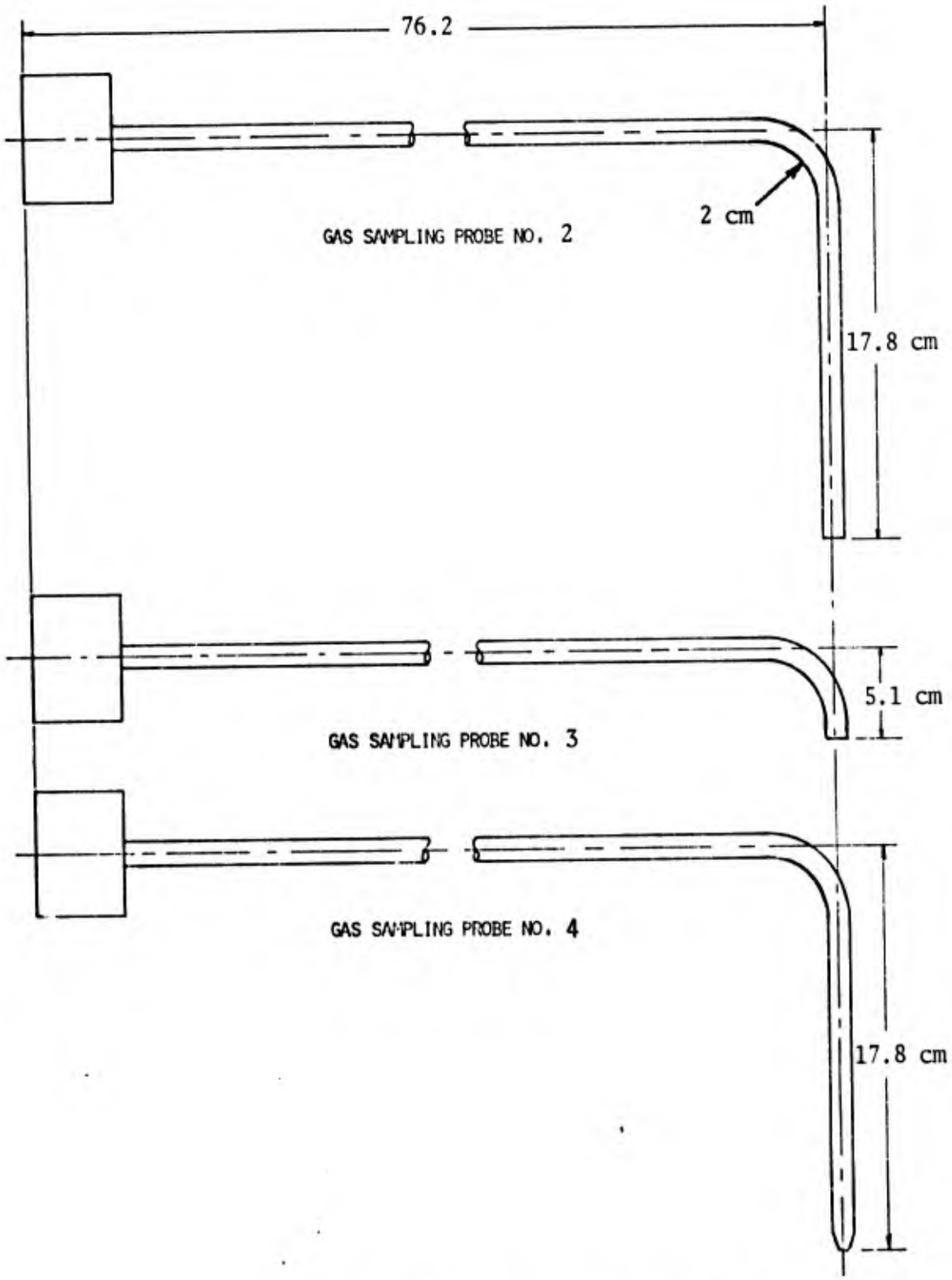

Figure 6. Three side entry probes

CL 952

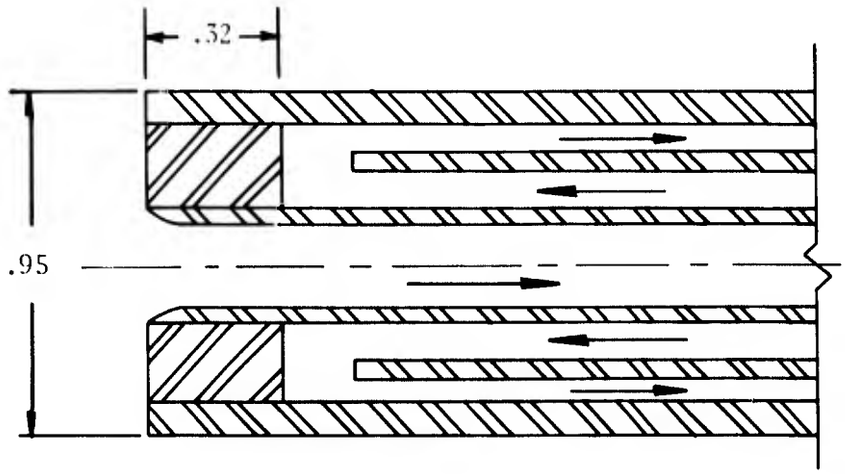

TIP CONFIGURATION FOR PROBES 1, 2, 3

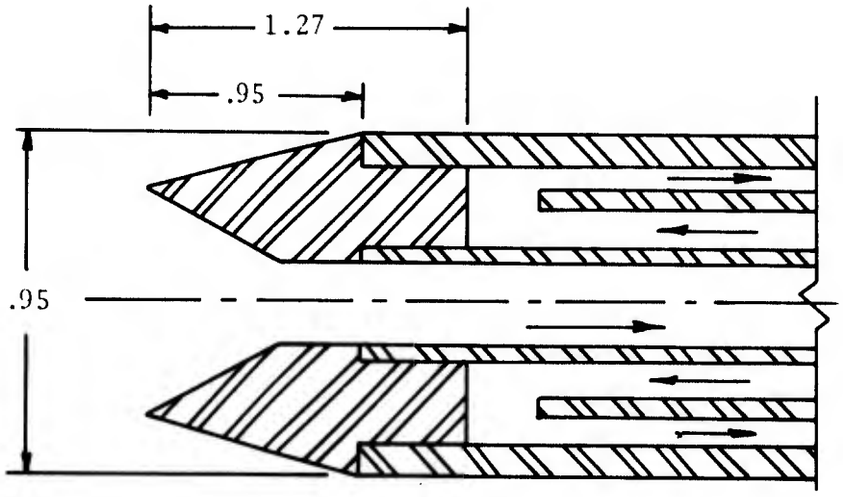

TIP CONFIGURATION FOR PROBE 4

Figure 7. Probe Tip Configurations (Dimensions in cm)

E. Run Conditions

As mentioned earlier, the present work is concerned with the same flame examined by Tuttle et al. (1975). Tuttle selected his operating conditions as being representative of a combustor operating at a cruise condition. Thus, the operating conditions for this study (and for the study by Tuttle et al. (1975)) are: pressure = 5 atmospheres, inlet temperature = 500^{o}K, air flow rate = 1.5 kg/sec, overall equivalence ratio = 0.2, and the fuel is liquid propane. The two axial sampling locations have been selected as being representative of conditions within the recirculation zone (2.54 cm downstream) and outside of this zone (8.89 cm downstream). The section which follows includes graphs and discussions of the radial pollutant profiles for both axial sampling locations.

SECTION IV

RESULTS

Results of this study are displayed in figures 8 through 15. These graphs show the variation of pollutant concentration with radial distance from the centerline of the combustor. Figures 8 through 11 pertain to sampling locations 2.54 cm downstream of the disc and figures 12 through 15 apply to tip positions 8.89 cm downstream. The data from each probe are graphed using a distinct symbol and the data from Tuttle et al. (1975) using probe #1 are included for comparison purposes. Superimposed on each of the pollutant profiles is a probe tip drawing which is in scale with the distances on the horizontal axis. This drawing is a reminder that spatial resolution is limited by probe diameter. There is little point in measuring pollutant concentrations at sampling points less than 0.5 cm apart when the probe diameter is nearly 1.0 cm.

Figures 8 and 12 show the variation of CO concentration with radial distance. Except near the outer edge of the CO profile at 2.54 cm, scatter is minimal. Especially noticeable is the agreement among the blunt tipped probes and the depressed CO concentrations obtained with the tapered tip probe. As expected, the scatter in the shear layer ($r \simeq 5.7$ cm) is more pronounced due to the already mentioned uncertainity in probe tip position. The plot for 8.89 cm also shows good agreement among the four probes, but the scatter is most pronounced at $r \simeq 3.2$ cm indicating that the shear layer is located there. The cross section of the combustor in figure 3 shows the two axial probe positions as well as the approximate shape of the

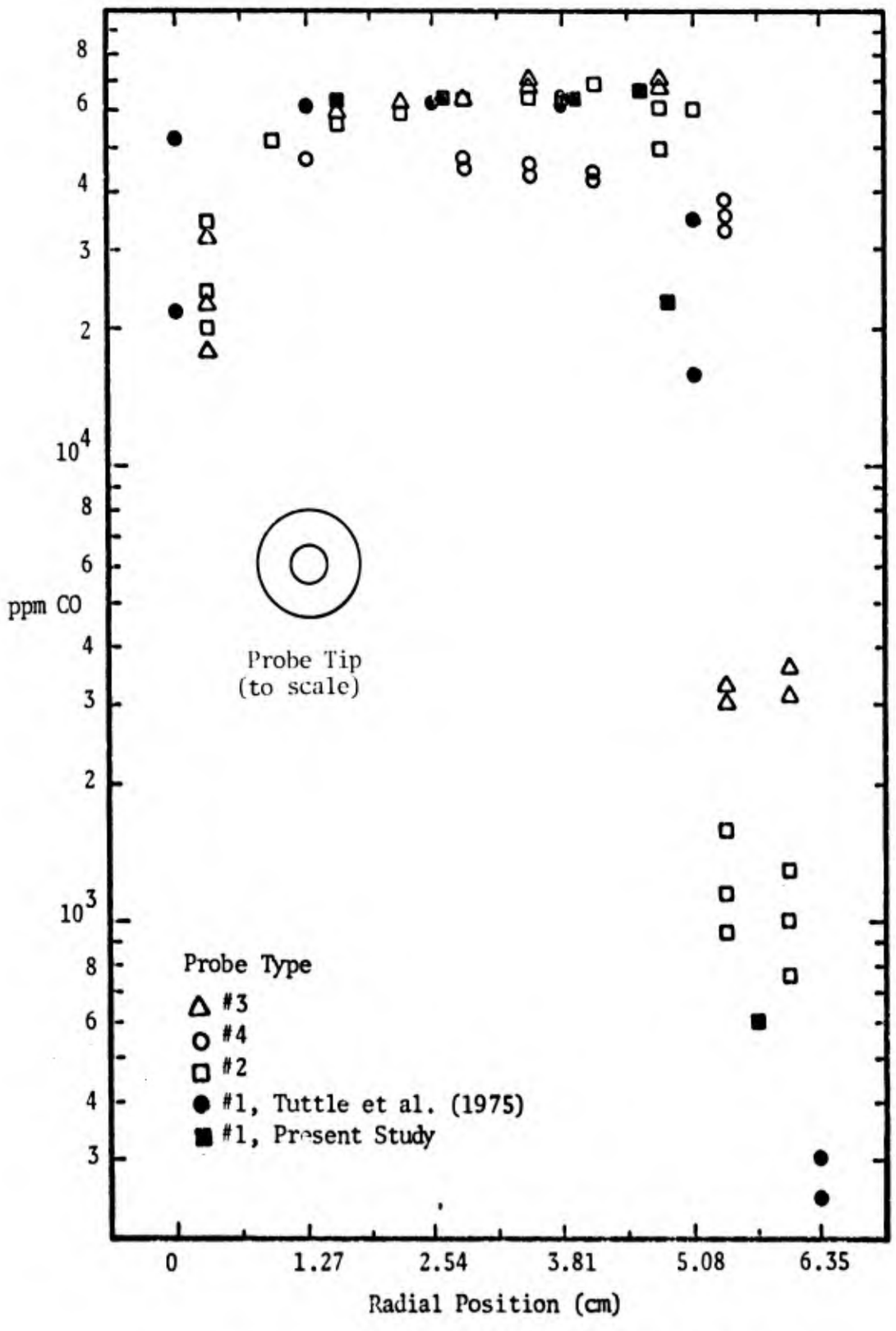

Figure 8. CO Concentration Profile at 2.54 cm

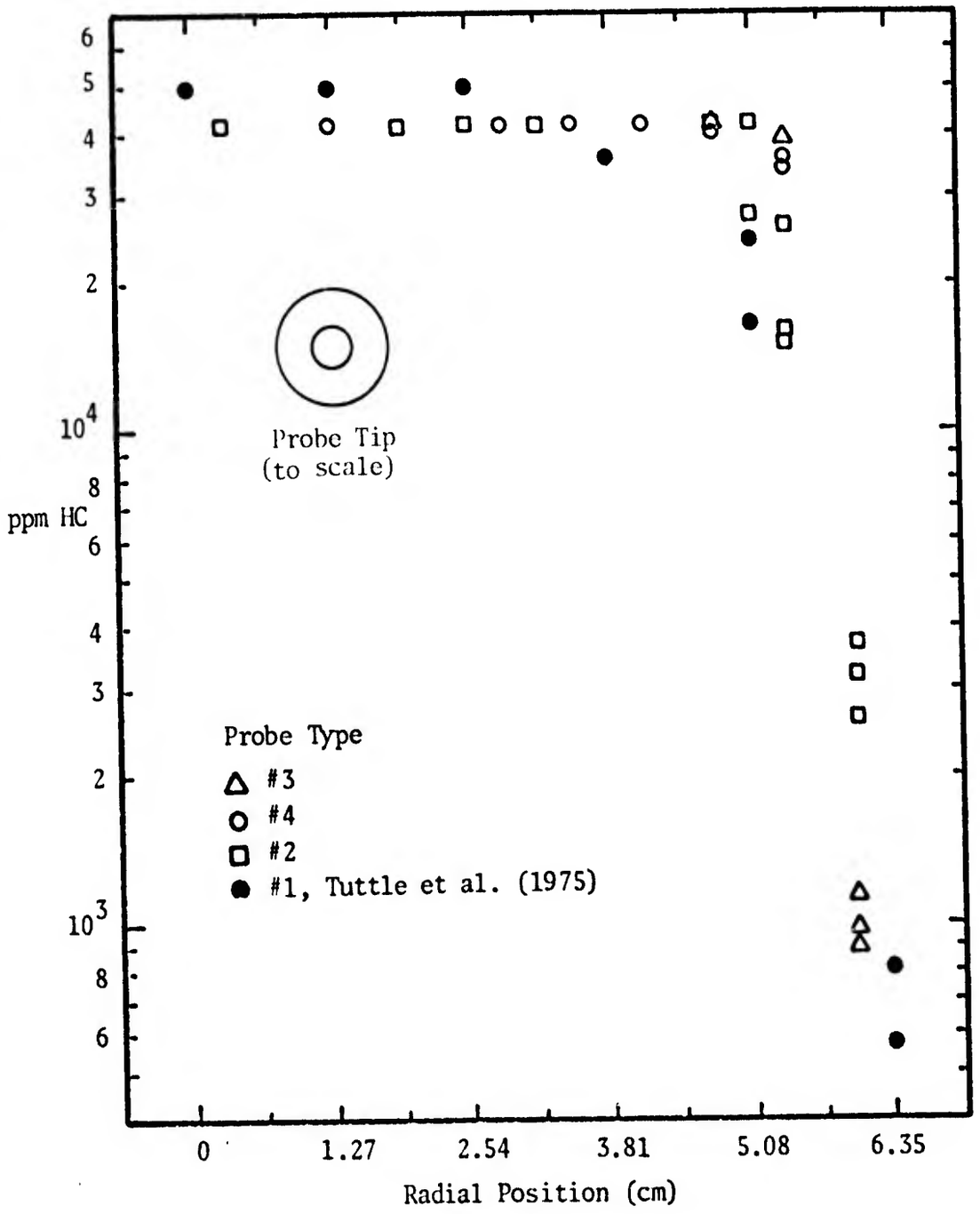

Figure 9. HC Concentration Profile at 2.54 cm

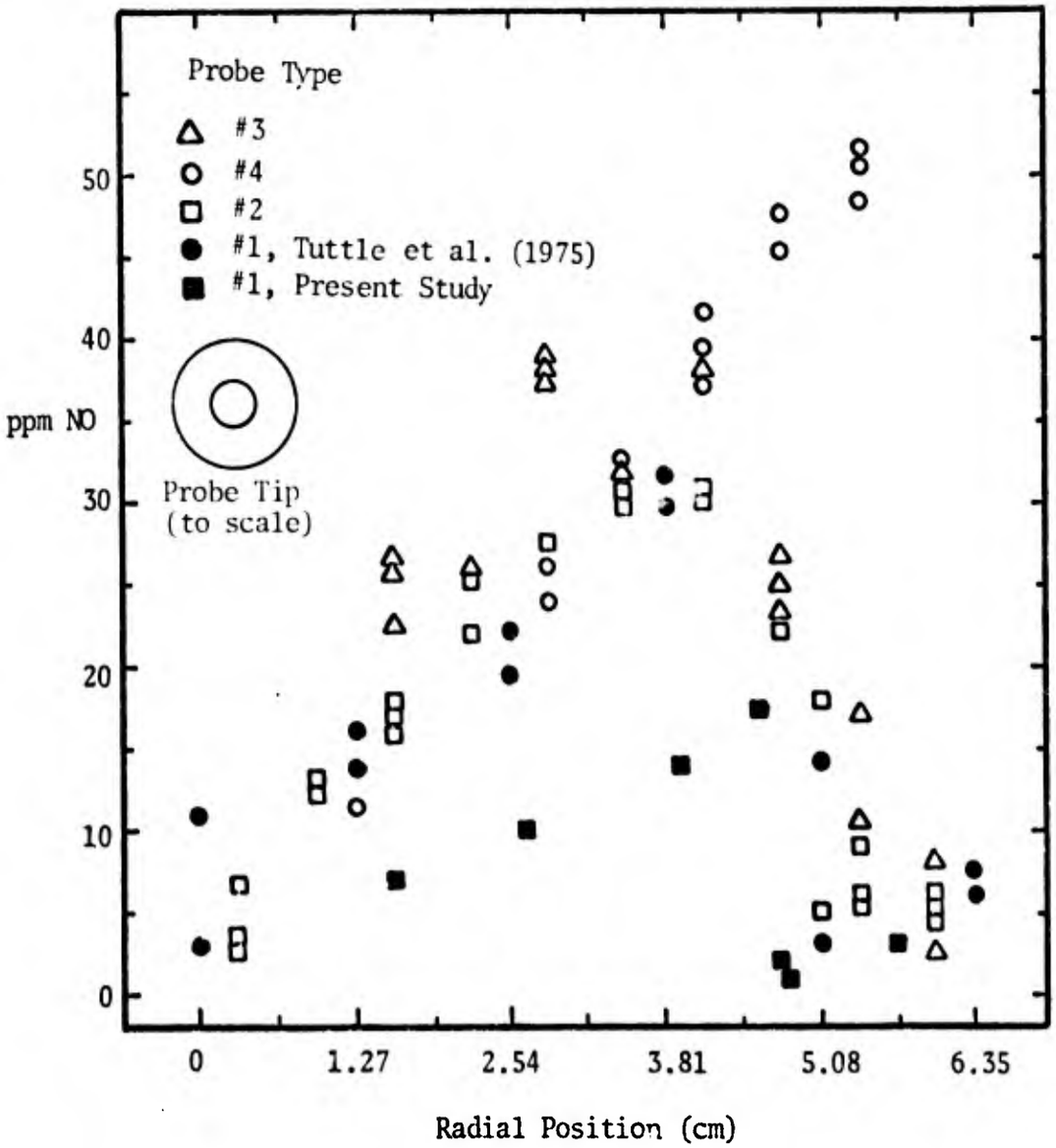

Figure 10. NO Concentration Profile at 2.54 cm

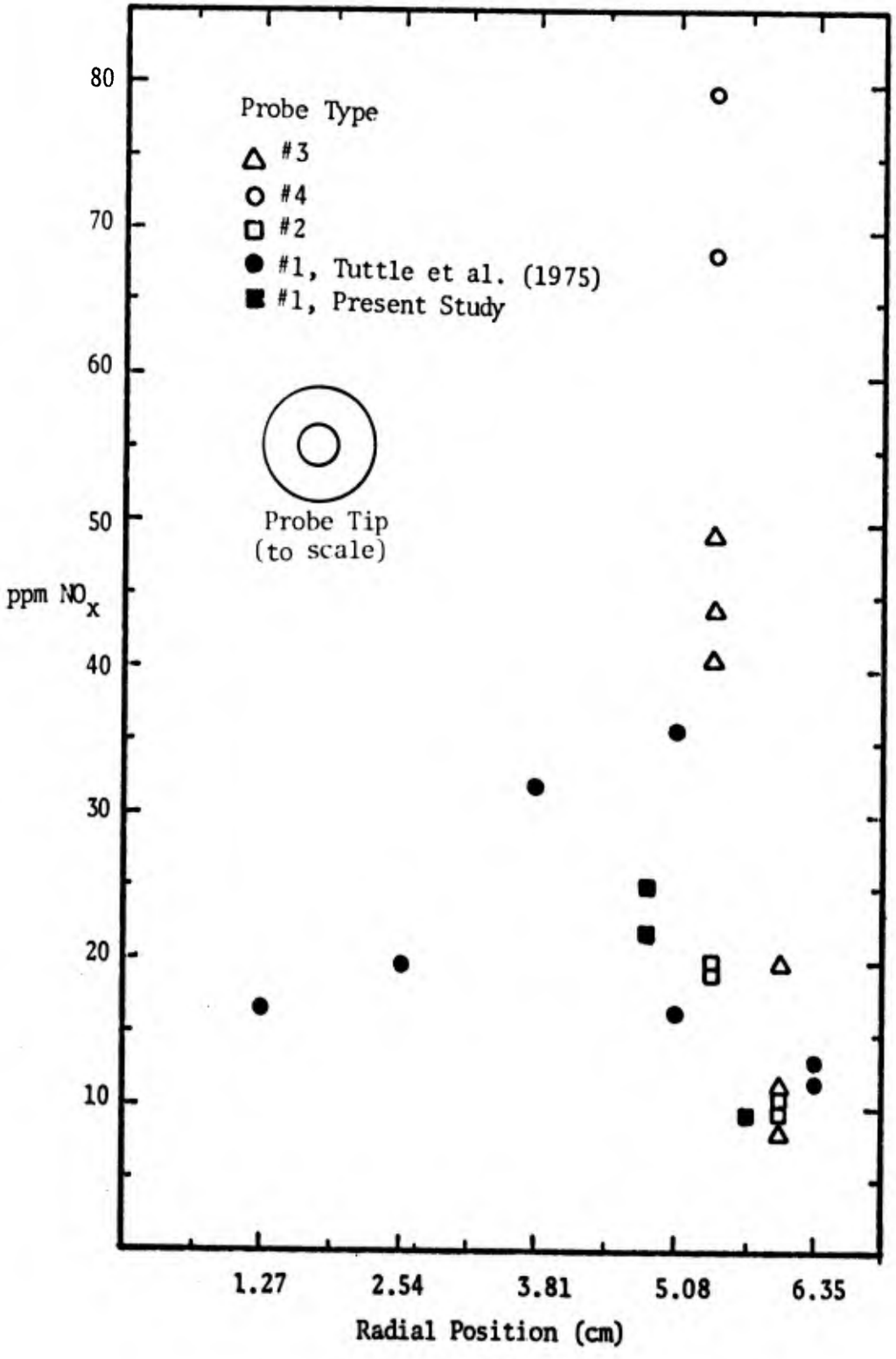

Figure 11. NO_x Concentration Profile at 2.54 cm

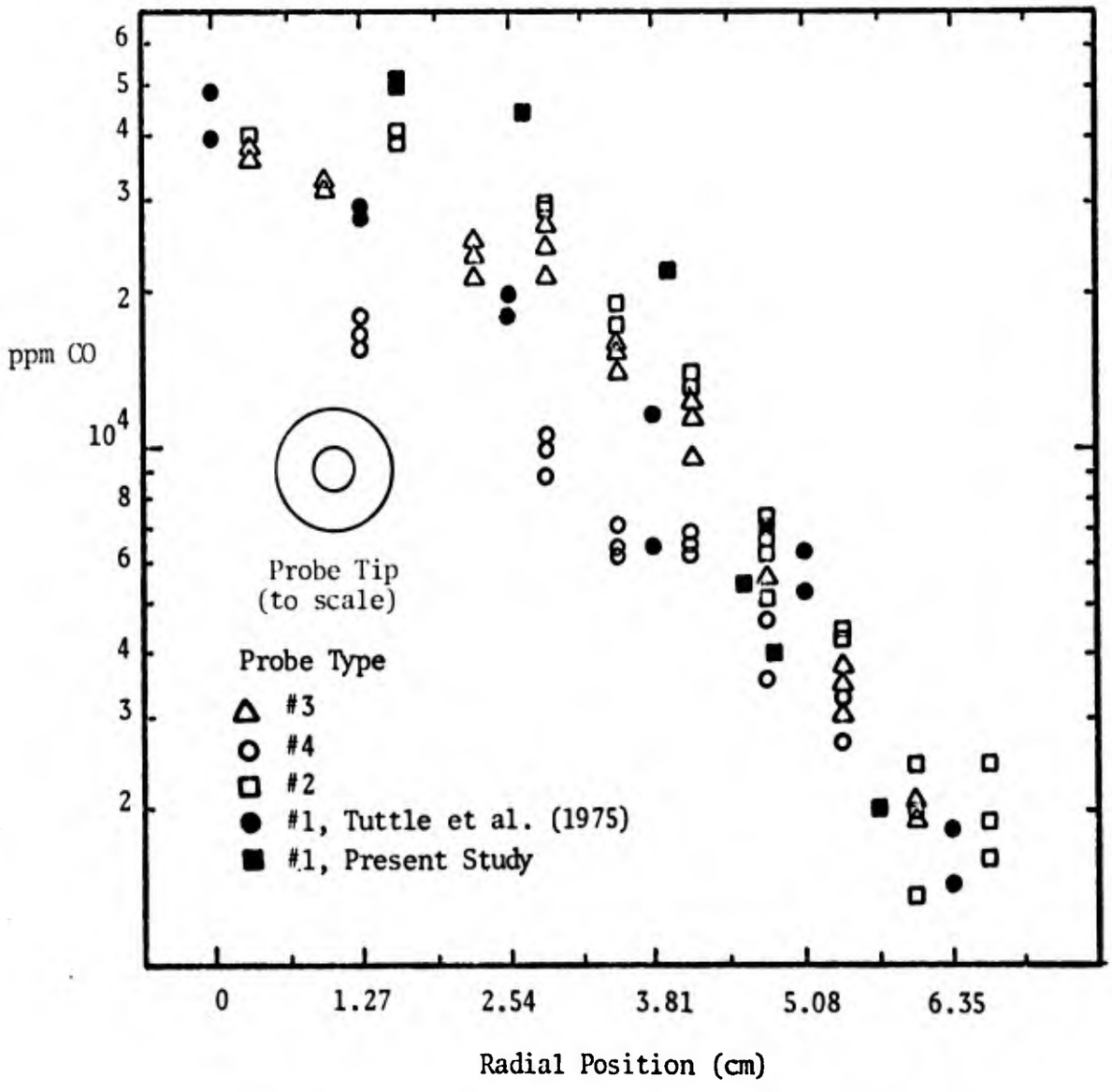

Figure 12. CO Concentration Profile at 8.89 cm

CL-1048

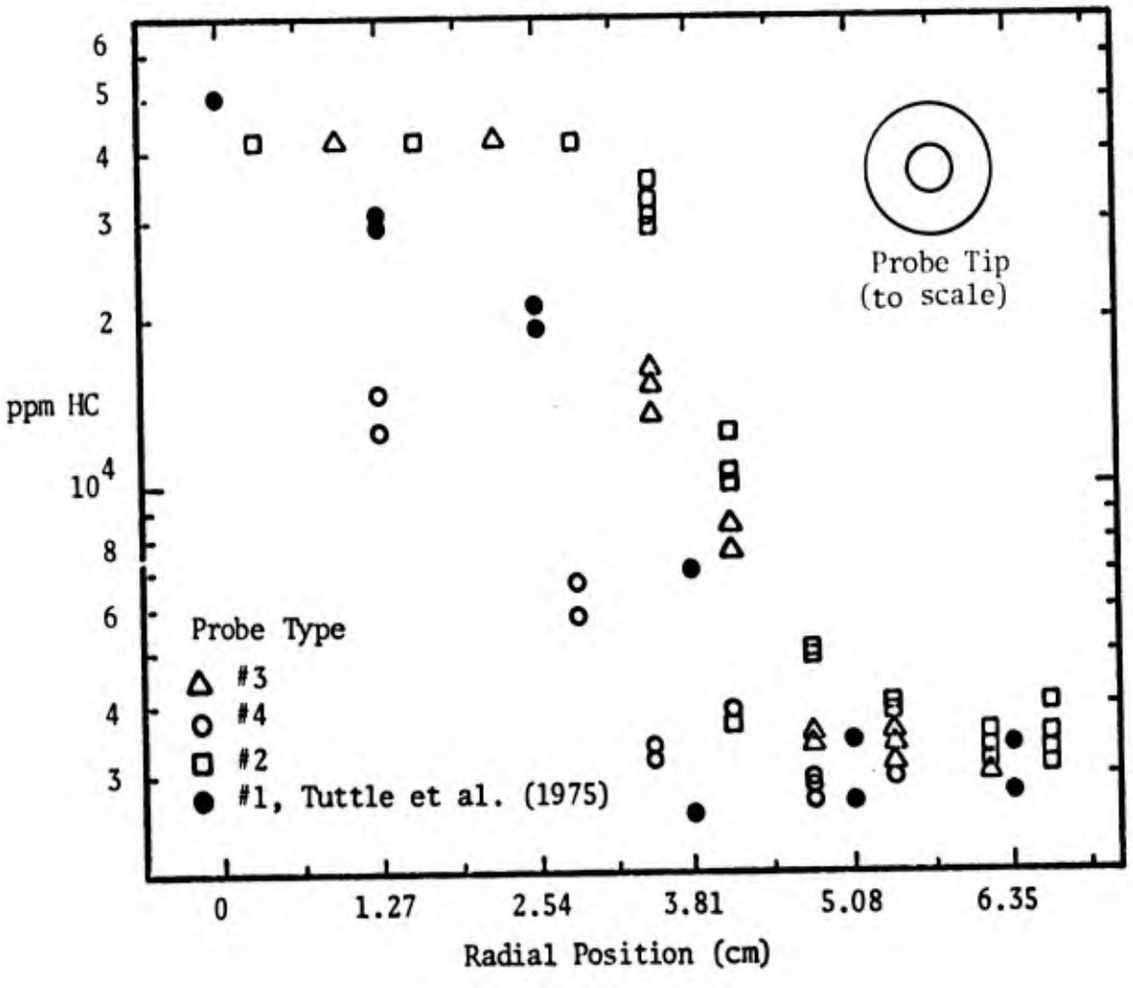

Figure 13. HC Concentration Profile at 8.89 cm

CL-1049

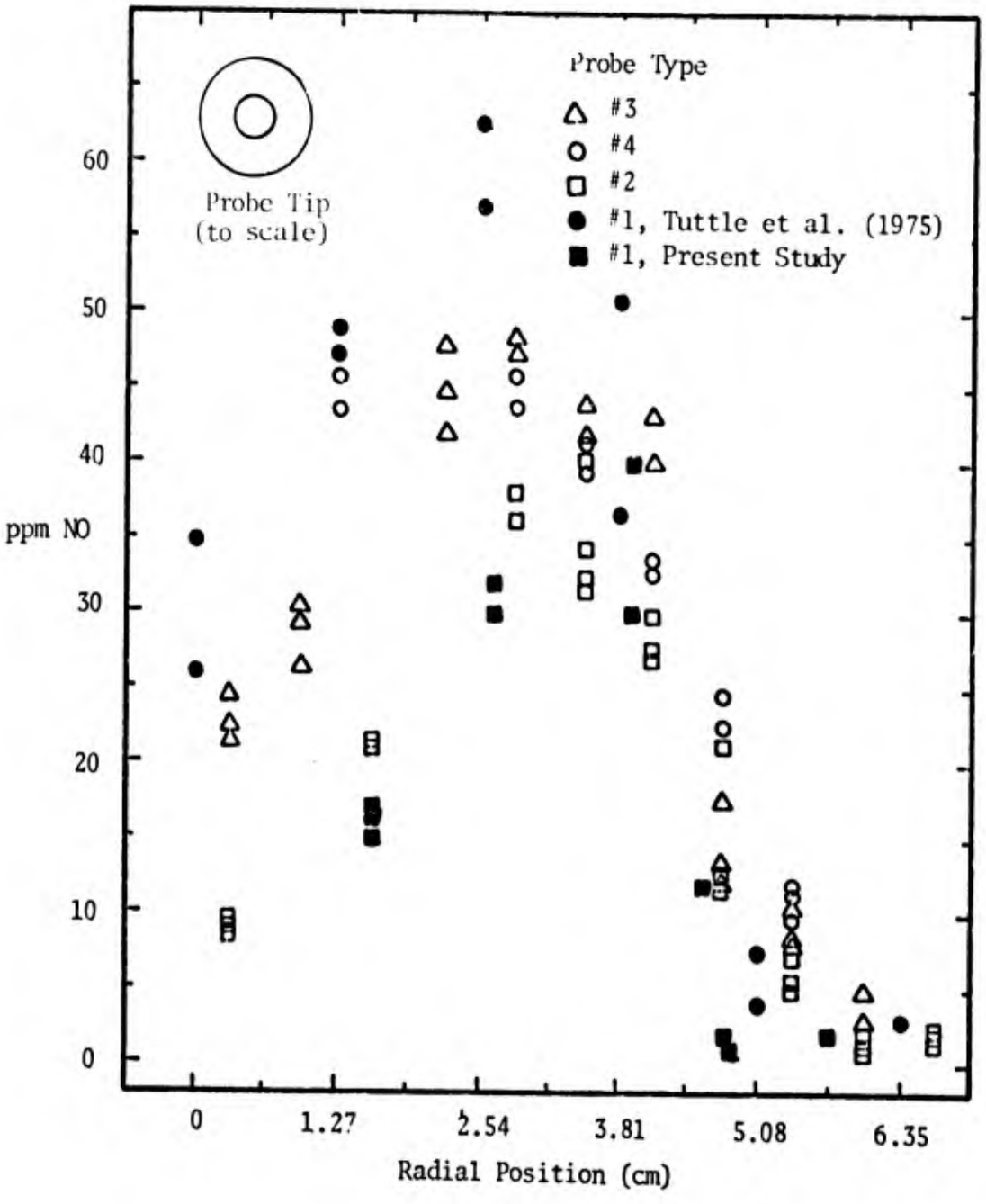

Figure 14. NO Concentration Profile at 8.89 cm

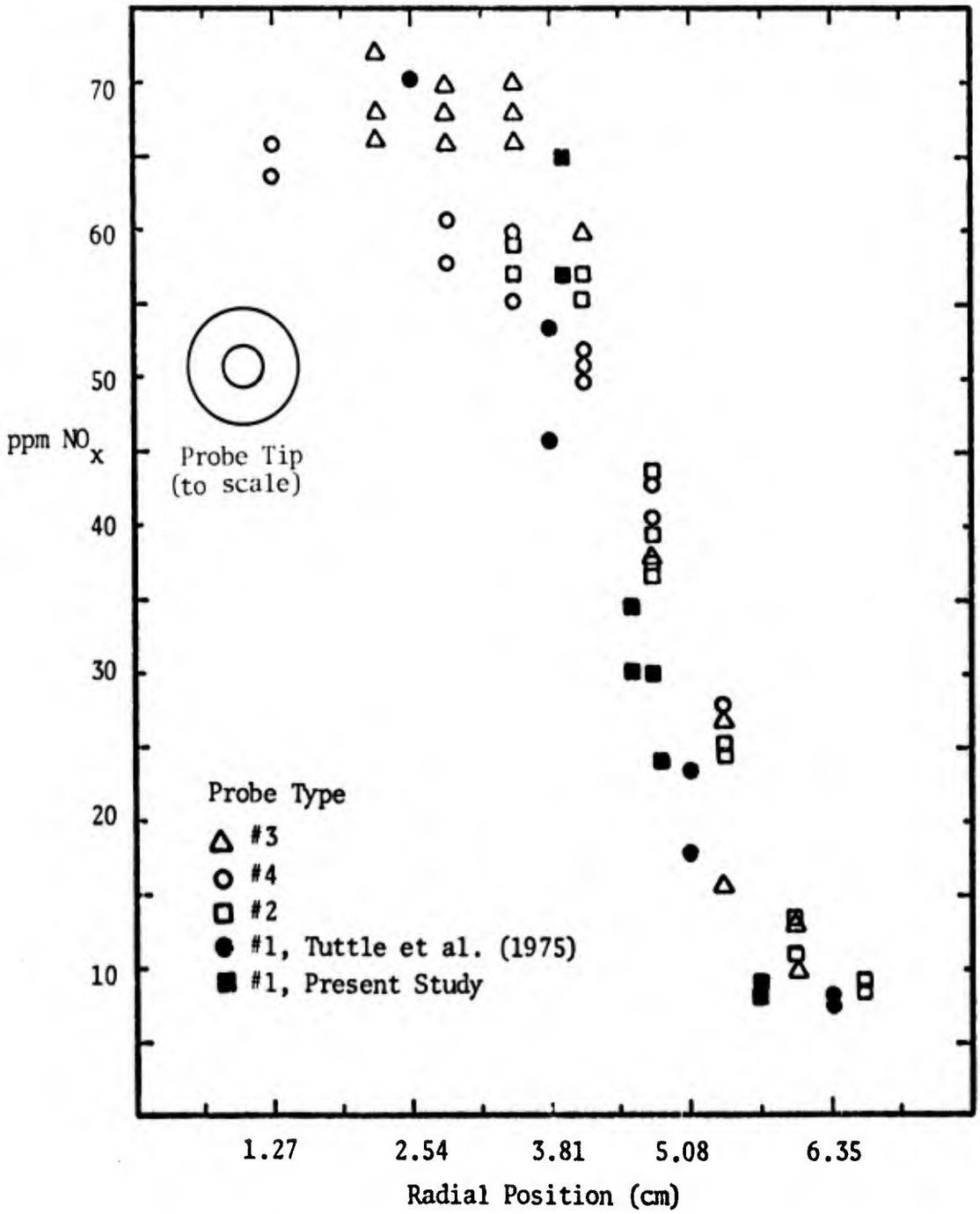

Figure 15. NO_x Concentration Profile at 8.89 cm

CL-1051

shear layer enclosing the recirculation zone. As shown, the recirculation zone extends one disc diameter downstream of the flameholder.

Figures 9 and 13 contain HC concentrations at the two axial sampling locations. Two comments should be made concerning these graphs. First, the lack of scatter at the 2.54 cm axial sampling location is deceptive because the hydrocarbon analyzer used in this study has been calibrated such that it becomes saturated for HC readings above 42,200 ppm. Thus, except for the data from Tuttle et al. (1975), all data above 40,000 ppm do not truly reflect the amount of HC present at that sampling location. Tuttle et al. (1975) calibrated their hydrocarbon analyzer to saturate at a level of 50,000 ppm, which indicates that Tuttle's data at 50,000 ppm are low. No similar analyzer saturation occurred with any of the other three pollutant species.

Second, during the early stages of this study, probe #1 was used to analyze pollutant concentrations in the quadrant above the centerline of the combustor. However, the resultant pollutant concentration profiles agreed poorly with those of Tuttle et al. (1975). It was later discovered that Tuttle had probed the quadrant below the centerline. Thus, probe #1 was reinserted to analyze the same lower quadrant, and it is that second probing with probe #1 which is shown in the pollutant profiles. Species concentrations measured by probe #1 in the upper quadrant are presented in Tables A-9 through A-12. Comparing the tabulated profiles for the upper and lower quadrants indicates that the shear layer is located approximately 3.8 cm from the centerline in the upper quadrant, and 5.7 cm from the centerline in the lower quadrant. Differing pollutant profiles from the two quadrants may reflect a

flowfield asymmetry which might be attributable to the temperature rake traversing the upper quadrant immediately upstream of the disc. The reason that no probe #1 data from the present study are presented in the HC plots is that the hydrocarbon analyzer was not functioning at the time of the second probing. Note in the HC and CO plots for x = 8.89 cm that the readings from the tapered tip probe are well below the readings from the other probes. These depressed readings are believed to be a tip effect and two possible explanations are given in the Introduction and Summary section.

Figures 10 and 14 present a change of NO concentration with radial distance. Again note that the radial location of the greatest scatter seems to correspond to the shear layer location. In the NO profile for x = 2.54 cm, the greatest scatter occurs for r ≃ 5.7 cm and in the profile for x = 8.89 cm, the scatter seems most severe at r ≃ 3.2 cm. Also note that near the center and outer edges of the upstream profile (r = 0 and r = 6.35 cm) the NO concentrations are below 10 ppm. Since the vitiated inlet air has NO concentrations of approximately 8 ppm, the day to day variation of NO in the inlet air could be largely responsible for scatter at those radial positions.

Though the probe #1 NO concentration profiles from the present study are at most radial positions below the NO levels measured using the other probes, this effect is attributed to soot. Because probe #1 is at least three years old while the other probes are new, probe #1 probably contains more soot than the new ones. Possibly, the excess soot in the older probe is responsible for converting NO to NO_2. Another explanation is that the relatively clean stainless steel walls of the newer probes act as catalysts for the $NO_2 \rightarrow NO$ reaction. In either case, total NO_x appears to be conserved because there is no disparity between the

new and old probe measurements of NO_x. Both the NO and NO_x results are to be expected in light of the NO-NO_2 discussion in the literature review section.

The NO_x profiles are shown in figures 11 and 15. Recall that a stainless steel catalytic converter will not convert NO_2 to NO in the presence of large amounts of hydrocarbons. Thus, no NO_x data are presented for most radial positions when the probe tips are located 2.54 cm downstream of the disc. The data which are available for that axial location again show that the most severe scatter is in the shear layer. The NO_x plot for x = 8.89 cm repeats the shear layer scatter of the previous pollutant profiles. Nonetheless, the agreement of NO_x concentrations from the four probes is good, as is the agreement with the results of Tuttle et al. (1975). A comparison of the NO and NO_x profiles reveals that the apparent percentage of NO_x in the form of nitric oxide varies between 35% and 90%.

To put the radial profiles into perspective, the fact that they pertain to sampling locations in or near the recirculation zone should be emphasized. Sampling points near the regions of large concentration gradients were purposely selected to rigorously test the effect of tip shape, probe entry point, and tip to body proximity. Tuttle et al. (1975) showed that pollutant measurement repeatability is much better at the exhaust plane than at sampling locations very close to the flameholder (see figure 16). If the sampling points had been located near the combustor exhaust plane (where concentration gradients are small and temperature is relatively low) differences in the pollutant levels measured with these four probes would be greatly reduced.

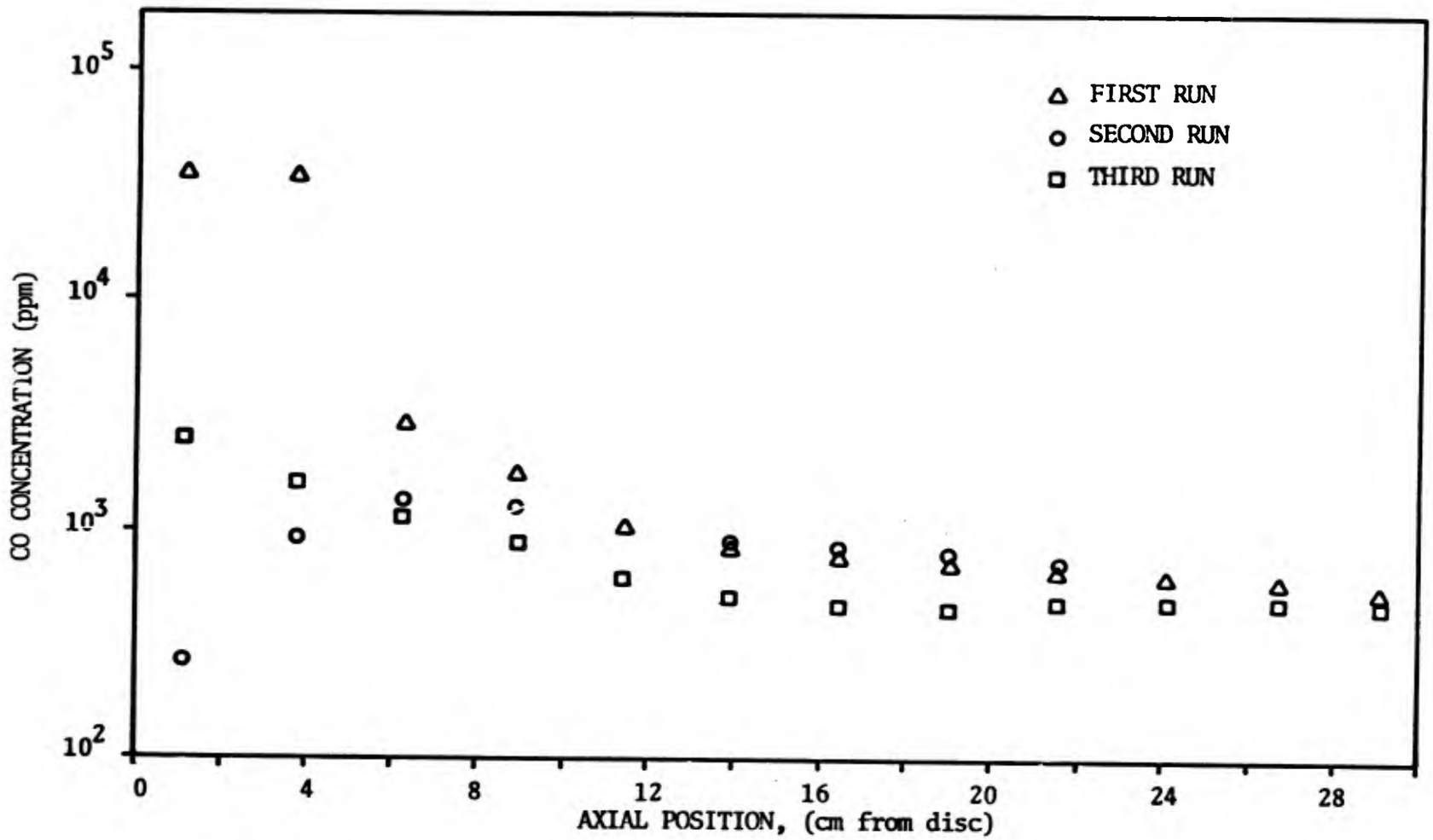

Figure 16. Axial CO Concentration Profile, 6.4 cm from Centerline
$\dot{m}_{air}$ = 1.0 kg/sec, ϕ_o = 0.1, P = 5 atm, T_{in} = 500°K (Tuttle et al., 1975)

A brief study of probe quench rate indicates that cooling water flowrate variation has a negligible effect on measured pollutant concentrations. During most of this probe comparison study, probe water flowrate is unrestricted by the cooling water valve, meaning that the valve is fully open. Probe water outlet temperature is monitored, but not controlled. Normally the probe outlet water temperature for probe #1 is approximately 330°K with a nearly constant inlet temperature of 297°K. When studying the effect of probe water flowrate variation, the control valve is closed until the temperature of the outlet water is just below the boiling point ($\simeq$ 370°K). Further reduction in the cooling water flows results in pure steam exiting the probe and this situation is avoided because of possible probe damage. Changes in pollutant concentrations due to probe water flowrate variation are either nonexistent or so small that they are lost in the data scatter.

Similarly, a variation of sample gas flowrate has no measurable effect on pollutant levels. Normally, the pollutant gas leaving the probe passes through a valve which is fully open and then enters a "Tee" in the sample line. One outlet of this Tee is a bypass line which is used to dump excess sample gas. The other outlet leg is the sample line leading to the gas analysis instruments, and pressure in this second leg is usually maintained at 9 psig by opening or closing a valve in the bypass line. To vary the sample gas flowrate, the bypass valve is completely closed and the valve at the probe exit is closed until pressure in the sample line leading to the instruments is again 9 psig. This reduction in sample gas flowrate results in no detectable change in pollutant concentrations.

One final note concerning the use of the side mounted probes involves the rather small radius, 90^{o} bend in each of these probes. Because of this bend, the three side entry probes are more susceptible to soot clogging than is the elbow mounted probe. Cleaning probe #1 is no problem using acetone and a 1/16 inch flexible brass rod. However, this rod will not negotiate the sharp bend of the side entry probes. Though cleaning probes #2, #3, #4 can still be accomplished by inserting the brass rod in both ends of the probe, the small radius bend makes the cleaning more difficult. Conclusions based on the results just discussed are the subject of the next section.

SECTION V

CONCLUSIONS

Four geometrically distinct, stainless steel probes, all water cooled, but not employing an aerodynamic quench, have been used to measure the pollutant levels within a simplified gas turbine combustor. Several radial positions at 2.54 cm and 8.89 cm downstream of the disc flameholder have been probed, and concentrations of CO, HC, NO, and NO_x have been measured.

Probe tip to body proximity and probe entry point have been found to have an imperceptible effect on these pollutant levels, within the data scatter. In contrast, probe tip geometry markedly affects the measurement of three of these pollutants. The tapered tip probe produces depressed HC and CO concentrations and elevated NO concentrations compared to the pollutant levels measured with the blunt tipped probes. Whether these altered pollutant concentrations are due to tip shape or tip temperature (the blunt tip is more effectively water-cooled than the tapered tip) has not been determined.

Regarding reproducibility, the results of this study have been compared with those from a similar study of the same flame by Tuttle et al. (1975). CO and HC have the most reproducible radial profiles and NO and NO_x are slightly less repeatable. The error involved with the reproduction of the pollutant concentrations in a high intensity, turbulent diffusion flame is not less than 10%.

APPENDIX

POLLUTANT CONCENTRATION DATA

The tables included in the Appendix contain the numerical values of the pollutant concentrations of CO, HC, NO and NO_x versus radial distance from the combustor centerline. Tables A-1 through A-8 contain the pollutant concentrations which are plotted in Figures 4-1 through 4-8. Tables A-9 through A-12 are unplotted pollutant levels from probe #1 sampling in the upper quadrant of the combustor (see discussion in Experimental Apparatus section). These final four tables are included for future reference only. A blank space in any Appendix table indicates the lack of pollutant concentration availability owing to either instrument malfunction or the incapability of measuring a pollutant concentration at the radial position. Every HC reading of 42,200 ppm indicates hydrocarbon analyzer saturation, meaning that the actual HC concentration at that radial position is greater than 42,200 ppm.

The data from Tables A-1 and A-5 were taken on 13, 18, 19, 21, September, 1978; Tables A-2 and A-6: 31, August and 1, 7, 25, 26, 28, September, 1978; Tables A-3 and A-7: 14, 15, 16, November, 1978; Tables A-4 and A-8: 21, 22, December, 1978; Tables A-9 and A-10: 24, 28, 29, August, 1978; and Tables A-11 and A-12: 20, 21, 22, November, 1978.

Pollutant levels for the vitiated air entering the test combustor were checked several times and found to average to the following values: 7.7 ppm NO; 11.4 ppm NO_x; 100 ppm HC; and 51.5 ppm CO.

TABLE A-1

AXIAL DISTANCE FROM FLAMEHOLDER = 2.54 cm, PROBE #3

Radial Distance from Centerline (cm)	CO (ppm)	HC (ppm)	NO (ppm)	NO_x (ppm)
6.03	3620	10,100	2.5	8.1
	3770	9720	4.3	11.6
	3170	8880	8.1	19.9
5.40	33,100	39,300	17.3	49.3
	30,400	38,900	10.7	40.7
	33,100	39,300	9.8	44.1
4.76	68,600	>42,200	23.4	----
	70,400	>42,200	25.1	----
	70,400	>42,200	26.8	----
4.13	72,300	>42,200	38.0	----
	68,600	>42,200	38.0	----
	68,600	>42,200	38.0	----
3.49	68,600	>42,200	30.3	----
	70,400	>42,200	32.9	----
	70,400	>42,200	32.0	----
2.86	63,400	>42,200	38.0	----
	65,100	>42,200	36.9	----
	65,100	>42,200	39.1	----
2.22	62,600	>42,200	25.1	----
	62,600	>42,200	25.1	----
	63,400	>42,200	25.1	----
1.59	60,000	>42,200	25.7	----
	60,000	>42,200	25.7	----
	60,000	>42,200	26.8	----
0.32	31,800	>42,200	4.4	----
	18,000	>42,200	2.1	----
	22,800	>42,200	4.4	----

TABLE A-2

AXIAL DISTANCE FROM FLAMEHOLDER = 2.54 cm, PROBE #2

Probe Radial Position (cm)	CO (ppm)	HC (ppm)	NO (ppm)	NO_x (ppm)
6.03	1300	37,200	4.3	10.6
	1000	32,100	6.2	----
	800	26,200	5.8	9.5
5.40	15,700	26,200	5.4	19.0
	9400	16,100	6.0	19.8
	11,500	15,200	9.1	19.4
4.76	61,700	>42,200	22.3	----
	61,700	>42,200	22.3	----
	50,400	>42,200	22.3	----
4.13	68,600	>42,200	31.0	----
	70,400	>42,200	29.9	----
3.49	65,100	>42,200	30.9	----
	63,400	>42,200	29.8	----
	65,100	>42,200	29.8	----
2.86	63,400	>42,200	27.6	----
	61,700	>42,200	27.6	----
	62,600	>42,200	24.3	----
2.22	60,000	>42,200	25.4	----
	60,000	>42,200	25.4	----
	60,000	>42,200	22.1	----
1.59	56,800	>42,200	15.8	----
	56,800	>42,200	17.9	----
	55,200	>42,200	17.0	----
0.95	50,400	>42,200	12.3	----
	52,000	>42,200	13.1	----
	52,000	>42,200	13.1	---
0.32	20,300	>42,200	2.7	----
	24,000	>42,200	3.6	----
	34,500	>42,200	6.7	----
-5.08	61,700	>42,200	17.9	----
	116,850	27,465	5.0	----

TABLE A-3

AXIAL DISTANCE FROM FLAMEHOLDER = 2.54 cm, PROBE #4

Probe Radial Position (cm)	CO (ppm)	HC (ppm)	NO (ppm)	NO_x (ppm)
5.40	35,900	35,900	48.4	68.3
	38,600	33,800	50.6	----
	33,100	33,800	51.7	79.4
4.76	35,600	40,100	47.8	----
	40,100	41,400	47.8	----
	40,100	41,400	45.6	----
4.13	44,400	>42,200	41.7	----
	43,000	>42,200	39.5	----
	43,000	>42,200	37.3	----
3.49	43,000	>42,200	32.5	----
	45,900	>42,200	32.5	----
	45,900	>42,200	30.3	----
2.86	47,400	>42,200	26.2	----
	45,900	>42,200	26.2	----
	47,400	>42,200	24.0	----
1.27	47,400	>42,200	13.9	----
	47,400	>42,200	11.7	----
	47,400	>42,200	13.9	----

TABLE A-4

AXIAL DISTANCE FROM FLAMEHOLDER = 2.54 cm, PROBE #1 (LOWER QUADRANT)

Probe Radial Position (cm)	CO (ppm)	HC (ppm)	NO (ppm)	NO_x (ppm)
5.71	1200	----	2.3	10.3
	1100	----	2.3	10.3
4.83	23,000	----	1.3	24.0
	23,000	----	1.3	20.0
4.75	51,000	----	1.8	----
4.57	67,000	----	15.5	----
	66,000	----	15.5	----
3.94	63,000	----	13.8	----
	63,000	----	14.0	----
2.67	63,000	----	10.6	----
	63,000	----	10.5	----
1.59	62,000	----	6.3	----
	60,500	----	6.7	----
	60,500	----	6.7	----

TABLE A-5

AXIAL DISTANCE FROM FLAMEHOLDER = 8.89 cm, PROBE #2

Probe Radial Position (cm)	CO (ppm)	HC (ppm)	NO (ppm)	NO_x (ppm)
6.67	2500	4000	2.5	11.0
	1600	3200	2.0	13.9
	1900	3500	1.7	14.1
	1600	3400	1.7	14.1
6.03	2400	3600	2.1	18.4
	2000	3400	1.6	18.4
	1400	3200	1.1	16.0
5.40	4400	4100	7.1	30.3
	4400	4000	5.5	29.4
	4300	4000	5.1	29.4
4.76	6300	4900	21.0	48.7
	7500	5100	11.4	41.6
	6800	5000	12.7	44.4
	5200	3700	12.5	42.5
4.13	14,000	12,700	26.8	60.2
	14,000	10,600	27.1	62.1
	13,200	10,100	29.6	60.2
3.49	19,200	35,900	40.1	64.0
	17,400	29,600	34.2	62.0
	19,200	33,400	32.3	62.0
2.86	29,100	>42,200	36.3	----
	29,100	>42,200	38.2	----
	30,400	>42,200	38.2	----
1.59	40,000	>42,200	21.0	----
	38,600	>42,200	21.0	----
	40,000	>42,200	21.4	----
.32	40,000	>42,200	9.6	----
	40,000	>42,200	9.0	----
	40,000	>42,200	8.8	----

TABLE A-6

AXIAL DISTANCE FROM FLAMEHOLDER = 8.89 cm, PROBE #3

Probe Radial Position (cm)	CO (ppm)	HC (ppm)	NO (ppm)	NO_x (ppm)
6.03	2000	3000	3.1	14.8
	2000	3400	2.7	18.0
	2100	3300	4.7	17.8
5.40	3800	3600	8.4	20.6
	3500	3500	10.3	29.8
	3000	3200	7.8	31.9
4.75	6500	3400	17.6	44.8
	5600	3500	12.3	42.9
	5600	3400	13.1	41.9
4.13	12,600	8500	43.2	64.7
	11,300	7600	40.1	64.7
	9500	5600	39.1	62.7
3.49	16,100	16,100	43.9	75.0
	15,600	15,200	43.9	71.1
	14,000	13,500	41.9	73.1
2.86	27,200	>42,200	47.3	70.9
	24,600	>42,200	48.3	72.9
	21,600	>42,200	48.3	75.1
2.22	23,400	>42,200	41.9	73.1
	25,300	>42,200	44.8	71.1
	21,600	>42,200	47.8	77.0
0.95	31,800	>42,200	26.3	----
	33,100	>42,200	29.3	----
	33,100	>42,200	30.2	----
0.32	35,900	>42,200	22.4	----
	37,200	>42,200	21.5	----
	37,200	>42,200	24.4	----

TABLE A-7

AXIAL DISTANCE FROM FLAMEHOLDER = 8.89 cm, PROBE #4

Probe Radial Position (cm)	CO (ppm)	HC (ppm)	NO (ppm)	NO_x (ppm)
5.40	3300	3000	10.7	33.7
	3200	3000	11.7	33.7
	2700	3400	9.7	34.7
4.76	4700	3000	22.6	43.6
	4700	2900	24.7	47.8
	3600	2700	24.7	45.7
4.13	6600	3800	32.7	56.7
	6960	4000	33.7	55.7
	6300	3800	32.7	54.7
3.49	7100	3400	39.4	64.5
	6500	3200	39.4	60.3
	6300	3400	41.5	60.3
2.86	9900	6800	45.7	65.8
	10,600	5900	43.7	63.7
	8800	5900	45.7	63.8
1.27	18,000	12,700	45.7	70.8
	15,700	12,700	46.6	68.7
	16,900	14,800	45.7	70.8

TABLE A-8

AXIAL DISTANCE FROM FLAMEHOLDER = 8.89 cm, PROBE #1 (LOWER QUADRANT)

Probe Radial Position (cm)	CO (ppm)	HC (ppm)	NO (ppm)	NO_x (ppm)
5.71	2200	----	2.2	12.9
	2300	----	2.1	16.0
4.83	4000	----	5.8	28.8
	4000	----	5.8	28.8
4.75	5800	----	8.5	35.0
4.57	5600	----	12.2	35.0
	5600	----	12.3	37.5
3.94	21,900	----	35.0	68.0
	21,900	----	27.0	62.0
2.67	46,100	----	27.0	----
	44,600	----	28.8	----
1.59	50,800	----	14.6	----
	49,200	----	16.7	----
	49,200	----	16.1	----

TABLE A-9

AXIAL DISTANCE FROM FLAMEHOLDER = 2.54 cm, PROBE #1 (UPPER QUADRANT)

Probe Radial Position (cm)	CO (ppm)	HC (ppm)	NO (ppm)	NO_x (ppm)
5.71	200	1300	7.7	9.9
	100	1200	7.5	9.3
4.44	500	1500	----	----
	400	1400	----	----
	500	1600	----	----
	500	1600	6.8	10.1
	500	1700	6.9	10.6
3.17	60,000	>42,200	40.9	----
	56,000	>42,200	43.0	----
	55,200	>42,200	38.8	----
1.90	66,900	>42,200	38.8	----
	65,100	>42,200	38.8	----
	66,900	>42,200	36.7	----
1.27	62,000	>42,200	28.3	----
	62,000	>42,200	30.3	----
	62,000	>42,200	31.2	----
0.63	60,000	>42,200	22.5	----
	63,400	>42,200	21.6	----

TABLE A-10

AXIAL DISTANCE FROM FLAMEHOLDER = 8.89 cm, PROBE #1 (UPPER QUADRANT)

Probe Radial Position (cm)	CO (ppm)	HC (ppm)	NO (ppm)	NO_x (ppm)
5.71	700	1900	7.8	9.9
	700	1800	6.8	11.3
	1100	2300	----	----
	1100	2100	----	----
	1000	2000	----	----
4.44	1600	1100	----	----
	1700	1400	----	----
	1600	1400	----	----
	1300	1400	15.7	25.5
	1300	1500	13.8	22.5
3.17	3400	1400	34.6	59.8
	2500	1500	53.4	64.0
	2400	1300	49.3	59.8
1.90	11,400	27,000	61.9	80.8
	12,500	28,700	64.0	89.2
	13,500	31,300	61.9	95.5
1.27	17,800	>42,200	59.5	79.0
	21,200	>42,200	51.7	67.3
	19,500	>42,200	55.6	106.2
0.63	38,600	>42,200	30.3	----
	41,500	>42,200	24.5	----

TABLE A-11

AXIAL DISTANCE FROM FLAMEHOLDER = 2.54 cm, PROBE #1 (UPPER QUADRANT)

Probe Radial Position (cm)	CO (ppm)	HC (ppm)	NO (ppm)	NO_x (ppm)
5.71	200	1400	3.1	5.7
	100	1200	3.3	8.4
	100	1300	3.3	8.6
4.44	600	1800	1.9	9.3
	500	1600	2.1	9.0
	600	1600	1.9	9.5
3.17	41,100	41,800	42.4	46.6
	41,100	41,800	44.5	53.1
	43,400	41,800	42.4	----
2.54	45,900	>42,200	41.2	----
	45,900	>42,200	39.0	----
	48,900	>42,200	34.7	----
1.90	55,200	>42,200	34.0	
	56,800	>42,200	35.9	----
	58,400	>42,200	33.8	----
0.63	53,600	>42,200	23.7	----
	52,000	>42,200	25.9	----
	52,000	>42,200	21.5	----

TABLE A-12

AXIAL DISTANCE FROM FLAMEHOLDER = 8.89 cm, PROBE #1 (UPPER QUADRANT)

Probe Radial Position (cm)	CO (ppm)	HC (ppm)	NO (ppm)	NO_x (ppm)
5.71	900	1700	1.6	9.9
	900	1800	0.8	9.3
	900	1700	0.8	9.9
4.44	1300	1400	1.9	17.5
	1300	1400	2.5	19.4
	1200	1300	2.7	19.0
3.17	2300	900	25.2	42.4
	2900	1200	27.4	46.6
	2900	1100	31.6	44.5
2.54	3000	1100	50.0	63.1
	2200	800	54.4	65.3
	2500	900	52.2	61.0
1.90	6000	4600	50.9	65.9
	7000	5100	53.1	65.9
	8300	5500	53.1	65.9
0.63	25,300	22,800	50.0	67.5
	24,000	20,300	50.0	67.5
	24,000	16,900	50.0	69.7

BIBLIOGRAPHY

Allen, J. D., (1975), "Probe sampling of oxides of nitrogen from flames," Combustion and Flame 24, 134-136.

Benson, R. and Samuelson, G. S., (1977), "Oxides of nitrogen transformation while sampling combustion products containing carbon monoxide, hydrogen, and hydrocarbons," Western States Section/Combustion Institute Paper 77-7.

England, Christopher, Houseman, J., and Teixeira, D. P., (1973), "Sampling nitric oxide from combustion gases," Combustion and Flame 20, 439-442.

Hilliard, J. C. and Wheeler, R. W., (1977), "Catalysed oxidation of nitric oxide to nitrogen dioxide," Combustion and Flame 29, 15-19.

Kramlich, John C. and Malte, Philip C., (1978), "Modeling and measurement of sample probe effects on pollutant gases drawn from flame zones," Combustion Science and Technology 18, 91-104.

LaPointe, C. W. and Schultz, W. L., (1971), "Measurement of nitric oxide formation within a multi-fueled turbine combustor, Emissions From Continuous Combustion Systems, W. Cornelius and W. G. Agnew, editors, 211-242, Plenum Press, N. Y.

Laurendeau, Normand M., (1975), "Fast nitrogen dioxide reactions: Significance during NO decomposition and NO_2 formation," Combustion Science and Technology 11, 89-96.

Schefer, R. W., Matthews, R. D., Cernansky, N. P., and Sawyer, R. F., (1973), "Measurement of NO and NO_2 in combustion systems," Western States Section/Combustion Institute Paper 73-31.

Seery, D. J., Zabielski, M. F., and Dodge, L. G., (1977), "Investigation of NOx, nitrate, and sulphate production in laboratory flames," EPA-600/7-77-073d, 209-234.

Tuttle, J. H., Shisler, R. A., and Mellor, A. M., (1974), "Nitrogen dioxide formation in gas turbine engines: Measurements and measurement methods," Combustion Science and Technology 9, 261-271.

Tuttle, J. H., Shisler, R. A., Bilger, R. W., and Mellor, A. M., (1975), "Emissions from aircraft fuel nozzle flames," PURDU-CL-75-04, School of Mech. Eng., Purdue University.

*U.S.Government Printing Office: 1979 — 657-002/122